© 2015. Published by The Company of Biologists Ltd | Development (2015) 142, 1146-1158 doi:10.1242/dev.113886

RESEARCH ARTICLE

The serpin PN1 is a feedback regulator of FGF signaling in germ layer and primary axis formation

Helena Acosta[1,*], Dobromir Iliev[1,*], Tan Hooi Min Grahn[1,*], Nadège Gouignard[1], Marco Maccarana[2], Julia Griesbach[1], Svende Herzmann[1], Mohsen Sagha[1,3], Maria Climent[1] and Edgar M. Pera[1,‡]

ABSTRACT

Germ layer formation and primary axis development rely on Fibroblast growth factors (FGFs). In *Xenopus*, the secreted serine protease HtrA1 induces mesoderm and posterior trunk/tail structures by facilitating the spread of FGF signals. Here, we show that the serpin Protease nexin-1 (PN1) is transcriptionally activated by FGF signals, suppresses mesoderm and promotes head development in mRNA-injected embryos. An antisense morpholino oligonucleotide against PN1 has the opposite effect and inhibits ectodermal fate. However, ectoderm and anterior head structures can be restored in PN1-depleted embryos when HtrA1 and FGF receptor activities are diminished, indicating that FGF signals negatively regulate their formation. We show that PN1 binds to and inhibits HtrA1, prevents degradation of the proteoglycan Syndecan 4 and restricts paracrine FGF/Erk signaling. Our data suggest that PN1 is a negative-feedback regulator of FGF signaling and has important roles in ectoderm and head development.

KEY WORDS: SerpinE2, HtrA1, Syndecan, FGF, Early development, *Xenopus*

INTRODUCTION

The question of how the body plan acquires proper proportioning of its germ layers and subdivides the primary axis into head, trunk and tail structures is of fundamental importance in developmental biology. In *Xenopus*, mesoderm formation occurs after the midblastula transition, when signals from the vegetal endoderm, primarily members of the Nodal-related class of the TGFβ family and Fibroblast growth factors (FGFs), induce mesoderm from competent ectoderm in the adjacent marginal zone (De Robertis et al., 2000; Kimelman, 2006). At the advanced gastrula stage, posterior mesoderm secretes signals such as Wnts and FGFs, but also Nodals and BMPs, that convert head into trunk and tail structures (Niehrs, 2004; Pera et al., 2014). The ectoderm and head are considered as default fates that form in the absence of growth factor signaling.

FGFs stimulate mesoderm induction and posterior development via the Extracellular signal-regulated kinase (Erk) pathway (Amaya et al., 1991; Umbhauer et al., 1995). Fgf4 and the T-box transcription factor *Xenopus* brachyury (Xbra) engage in a positive feedforward loop that causes amplification of the mesoderm-inducing and posteriorizing signal (Isaacs et al., 1994; Schulte-Merker and Smith, 1995). Although negative-feedback mechanisms for FGF signals exist in the mesoderm (Böttcher and Niehrs, 2005), it is not clear how the ectoderm protects itself against self-propagating FGF signals. Whether FGF signals need to be suppressed to allow head formation has not convincingly been demonstrated.

Proteoglycans through their heparan sulfate (HS) chains capture FGFs at the cell surface, regulate their extracellular transport to target cells and participate in complex formation with their receptors (Yu et al., 2009; Matsuo and Kimura-Yoshida, 2013). We previously described an autoinductive loop of FGF and the secreted serine protease HtrA1 that leads to the mobilization of FGF/proteoglycan complexes and long-range FGF signaling during mesoderm induction and posteriorization in *Xenopus* embryos (Hou et al., 2007). FGFs stimulate *HtrA1* transcription also in the chick (Ferrer-Vaquer et al., 2008) and zebrafish (Kim et al., 2012). It is apparent that the proteolytic activity of HtrA1 needs to be regulated to protect the integrity of proteoglycans and ensure proper FGF signaling in the embryo.

In a direct screen for secreted proteins in early *Xenopus* embryos, we identified Protease nexin-1 (PN1) (Pera et al., 2005). PN1, which is also known as Glial-derived nexin or SerpinE2, is a serine protease inhibitor (serpin) that contains an exposed reactive center loop (RCL) that covalently binds to and blocks proteases such as thrombin, plasminogen activator, trypsin, urokinase and factor XIa (Baker et al., 1980; Stone et al., 1987; Knauer et al., 2000). Serpins inhibit target proteases through a suicide substrate mechanism, by which the protease cleaves the RCL at the process site and forms a covalent acyl-enzyme complex that causes irreversible inhibition of the protease (Olson and Gettins, 2011; Li and Huntington, 2012). *PN1* null mice exhibit increased proliferation in the postnatal cerebellum (Vaillant et al., 2007), but no apparent early developmental defects have been described. In *Xenopus* embryos, overexpression of PN1 inhibits convergence extension movements and the expression of mesendodermal markers (Onuma et al., 2006). Here, we show that *PN1* gene activity is positively regulated by FGF signals and is crucial for the formation of ectoderm and head structures. We report that PN1 binds and inhibits HtrA1, regulates the turnover of Syndecan 4 (Sdc4) and controls the range of FGF/Erk signaling. Thus, our study uncovers a novel important role of PN1 as negative-feedback regulator in the extracellular regulation of the HtrA1-FGF axis during germ layer and primary axis development in *Xenopus*.

RESULTS

Two *Xenopus PN1* genes are partially co-expressed with *HtrA1* and activated by FGF signals

In a screen for secreted proteins from gastrula stage *Xenopus laevis* embryos, we previously isolated five non-redundant full-length

[1]Lund Stem Cell Center, Lund University, Lund 221 84, Sweden. [2]Department of Experimental Medical Science, Lund University, Lund 221 84, Sweden. [3]Department of Anatomical Sciences and Pathology, School of Medicine, Ardabil University of Medical Sciences, Ardabil 56189-53141, Iran.
*These authors contributed equally to this work

‡Author for correspondence (edgar.pera@med.lu.se)

Received 18 June 2014; Accepted 27 January 2015

Development (2015) 142, 1146-1158 doi:10.1242/dev.113886

cDNA clones that encode the serpin family member PN1 (Pera et al., 2005). PN1 appeared as a 45 kDa protein in the supernatant of transfected and [^{35}S]methionine/cysteine-labeled HEK293T cells (Fig. 1A). Using NCBI BLAST, we identified a second *X. laevis PN1* (here referred to as *PN1.b*) that differs slightly from the originally identified *PN1.a* homeolog by 4% in derived amino acid sequence (supplementary material Fig. S1).

We compared the gene expression of *PN1.b*, the previously described *PN1.a* (Pera et al., 2005; Onuma et al., 2006) and the secreted serine protease *HtrA1* (Hou et al., 2007). RT-PCR and whole-mount *in situ* hybridization analyses reveal maternal and zygotic transcription of *PN1.a* and *PN1.b*, whereas *HtrA1* is robustly expressed only after the midblastula transition (Fig. 1B-K′; supplementary material Fig. S2A-H). At stage 10, all three genes were expressed in the animal cap and marginal zone (Fig. 1C-E; supplementary material Fig. S2C,D). At stage 13, they overlapped in the anterior neural plate, while *HtrA1* showed an additional unique domain in the posterior mesoderm (Fig. 1F-H′). In tailbud embryos, transcripts of both *PN1* homeologs were found in the notochord (Fig. 1I-J′). Interestingly, *PN1.b* was also robustly expressed in migrating neural crest cells, the ear placode and spinal cord, where *PN1.a* was less abundant or absent, suggesting differential regulation at this stage. *HtrA1* transcripts were localized in the notochord region and migrating neural crest cells (Fig. 1K,K′).

The gene expression patterns of *PN1* and *HtrA1* partially overlap with those of several FGFs and FGF receptors (Lea et al., 2009) and coincide with sites of FGF/Erk activation (Christen and Slack, 1999) in the marginal zone, anterior neural plate, notochord, ear placode and branchial arches, suggesting a possible interaction. In mRNA-injected embryos and animal cap explants at stage 10, *Fgf4* activated whereas the dominant-negative FGF receptor-1 construct *XFD* (Amaya et al., 1991) downregulated *PN1.a* and *PN1.b* transcription (Fig. 1L-O; supplementary material Fig. S2I-K), suggesting that FGF signals stimulate the expression of both *PN1* homeologs.

PN1 requires an intact RCL to restrict mesoderm, reduce neuronal differentiation and stimulate anteriorization

We injected synthetic mRNA of *PN1.a* (hereafter called *PN1*) into *Xenopus* embryos (Fig. 2). It was previously shown that marginal injection of *PN1* causes exogastrulation (Onuma et al., 2006). We observed that, upon animal injection of *PN1* mRNA, embryos underwent normal gastrulation but developed increased head structures and a shortened trunk-tail axis (Fig. 2A,B; supplementary material Fig. S3A,B). The eyes of *PN1*-injected tadpoles exhibited an expansion of the optic fissure known as coloboma. We obtained similar

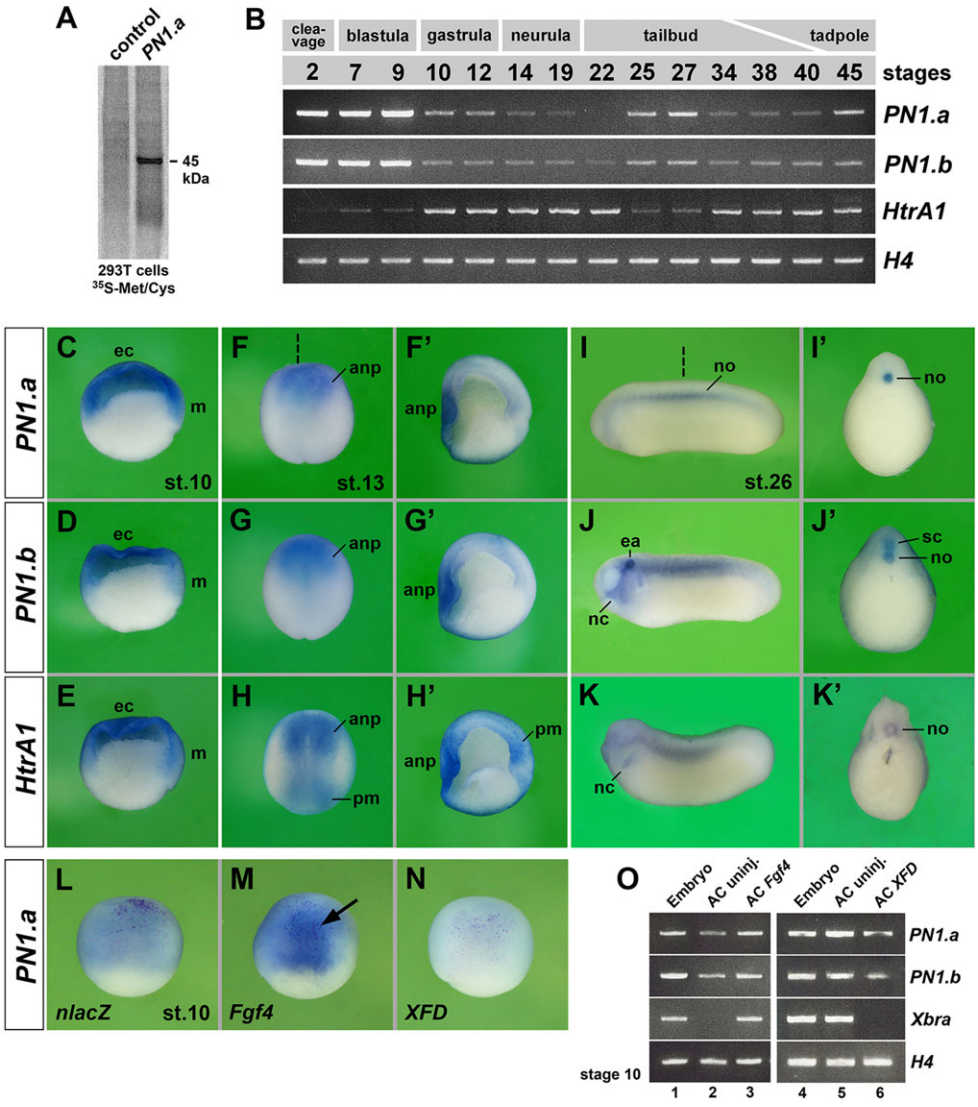

Fig. 1. Isolation and expression of *Xenopus PN1*. (A) SDS-PAGE of supernatant from transfected and [^{35}S] methionine/cysteine-labeled HEK293T cells. The 45 kDa band corresponds to secreted PN1.a protein. (B) RT-PCR of *PN1.a*, *PN1.b* and *HtrA1* in *Xenopus* embryos. *Histone H4* was used for normalization. (C-K′) Whole-mount *in situ* hybridization of *PN1.a*, *PN1.b* and *HtrA1* at stage 10 (C-E, hemisections), stage 13 (F-H, dorsal views; F′-H′, hemisections) and stage 26 (I-K, lateral views; I′-K′, transverse sections). Dashed lines indicate section planes. anp, anterior neural plate; ea, ear; ec, ectoderm; m, mesoderm; nc, neural crest; no, notochord; pm, posterior mesoderm; sc, spinal cord. (L-N) Lateral view of stage 10 embryos. A single injection of 9 pg *Fgf4* mRNA stimulates (arrow) and 450 pg *XFD* mRNA downregulates *PN1.a* expression. *nlacZ* mRNA was co-injected as lineage tracer (red nuclei). The frequency of embryos with the indicated phenotypes was: L, 67/67; M, 57/63; N, 47/53. (O) RT-PCR of *PN1.a* and *PN1.b* in animal cap (AC) explants injected with 12 pg *Fgf4* and 4.5 ng *XFD* mRNA (*n*=3 replicates).

Development (2015) 142, 1146-1158 doi:10.1242/dev.113886

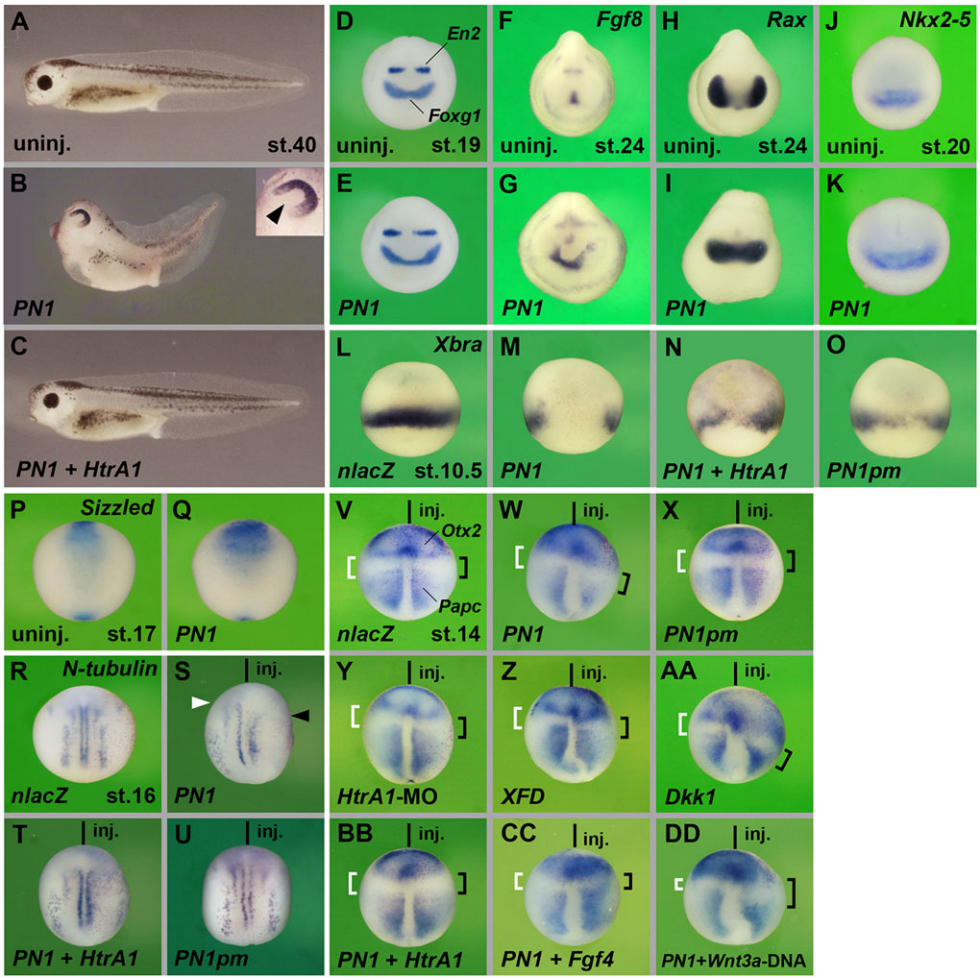

Fig. 2. PN1 promotes anterior development, suppresses mesoderm and reduces neuronal differentiation. (A) Uninjected tadpole embryo. (B) Injection of *PN1* mRNA induces enlargement of head structures and coloboma (arrowhead in inset). (C) Co-injection of *PN1* and *HtrA1* mRNA restores normal development. (D-K) Whole-mount *in situ* hybridization of post-neurula embryos in anterior view. *PN1* causes enlargement of the *Foxg1*, *En2*, *Fgf8* and *Nkx2-5* expression domains. *Rax* expression is not split into bilateral domains. (L-O) *Xbra* expression in early gastrulae, lateral view. A single marginal injection of *PN1* strongly reduces *Xbra* expression (M). *PN1* and *HtrA1* partially revert this effect (N). *PN1pm* mRNA causes only mild or no reduction of *Xbra* expression (O). (P,Q) Ventral view of neurulae. *PN1* expands anterior *Sizzled* expression. (R-X,BB) Dorsal view of neurula embryos. A single injection of *PN1* causes reduction and posteriorward retraction of *N-tubulin* (arrowheads in S), reduction of *Papc* and expansion of *Otx2* expression (brackets in W) on the targeted right side. *PN1* and *HtrA1* rescue these effects (T,BB). *PN1pm* does not affect these markers (U,X). (Y-AA) Injection of 15 ng *HtrA1*-MO, *XFD* mRNA or *Dkk1* mRNA also causes anteriorization. (CC) *Fgf4* mRNA rescues anteriorization by *PN1*. (DD) pCS2-*Wnt3a* (*Wnt3a*-DNA) reverts *PN1*-induced *Otx2* expansion, but not *Papc* reduction. Total mRNA amounts were: *PN1* constructs, 4 ng (1 ng in W,X,BB-DD, 16 ng in E,K,Q); *HtrA1*, 100 pg; *XFD*, 80 pg; *Dkk1*, 8 pg; *Fgf4*, 0.3 pg. Indicated phenotypes were shown by: B, 44/56; C, 30/30; E, 19/21; G, 16/16; I, 13/15; K, 14/17; M, 71/73; N, 18/32; O, 23/32; Q, 9/19; S, 41/42; T, 16/19; U, 42/42; W, 57/62; X, 31/39; Y, 20/24; Z, 27/31; AA, 59/60; BB, 19/23; CC, 19/24; DD, 15/16.

results with *PN1.b* mRNA (supplementary material Fig. S3C,E). In post-neurula embryos, *PN1* mRNA widened the expression domains of the telencephalic marker *Foxg1* and the posterior midbrain marker *En2*, expanded *Fgf8* in the hatching gland, frontal plate and the midbrain-hindbrain boundary, and delayed the splitting of the *Rax*-positive eye field into distinct bilateral domains (Fig. 2D-I). *PN1* mRNA also enlarged expression of the heart marker *Nkx2-5* and the anterior domain of *Sizzled* in the ventral mesoderm (Fig. 2J,K,P,Q). Marginal injection of *PN1* mRNA caused loss of the pan-mesodermal marker *Xbra* in early gastrula embryos (Fig. 2L,M) (Onuma et al., 2006). At the neurula stage, animally injected *PN1* mRNA led to a reduction and posteriorward retraction of the neuronal differentiation marker *N-tubulin* and the trunk mesoderm marker *Papc*, whereas the anterior ectoderm marker *Otx2* was expanded (Fig. 2R,S,V,W; supplementary material Fig. S7A, B), underscoring its anteriorizing activity.

To investigate the impact of the serpin-specific RCL on PN1 activity, we generated a point mutation in PN1 (PN1pm), in which the critical arginine and serine residues at its process site are changed to proline (R362P and S363P; Fig. 3A). Microinjection of *PN1pm* mRNA caused only mild reduction of *Xbra* (Fig. 2O) (Onuma et al., 2006) and did not affect *N-tubulin*, *Papc* or *Otx2* expression (Fig. 2U,X), supporting the importance of an intact RCL for PN1 patterning activity.

HtrA1, FGF and Wnt signals can rescue PN1 activities

We realized that several effects of PN1 overexpression, including coloboma, loss of mesodermal *Xbra* expression and reduction of *N-tubulin*-positive neurons, are similar to phenotypes resulting from knockdown of HtrA1 (Hou et al., 2007) or suppression of FGF receptor activities (Amaya et al., 1991; Hardcastle et al., 2000). Moreover, anteriorization also

Development (2015) 142, 1146-1158 doi:10.1242/dev.113886

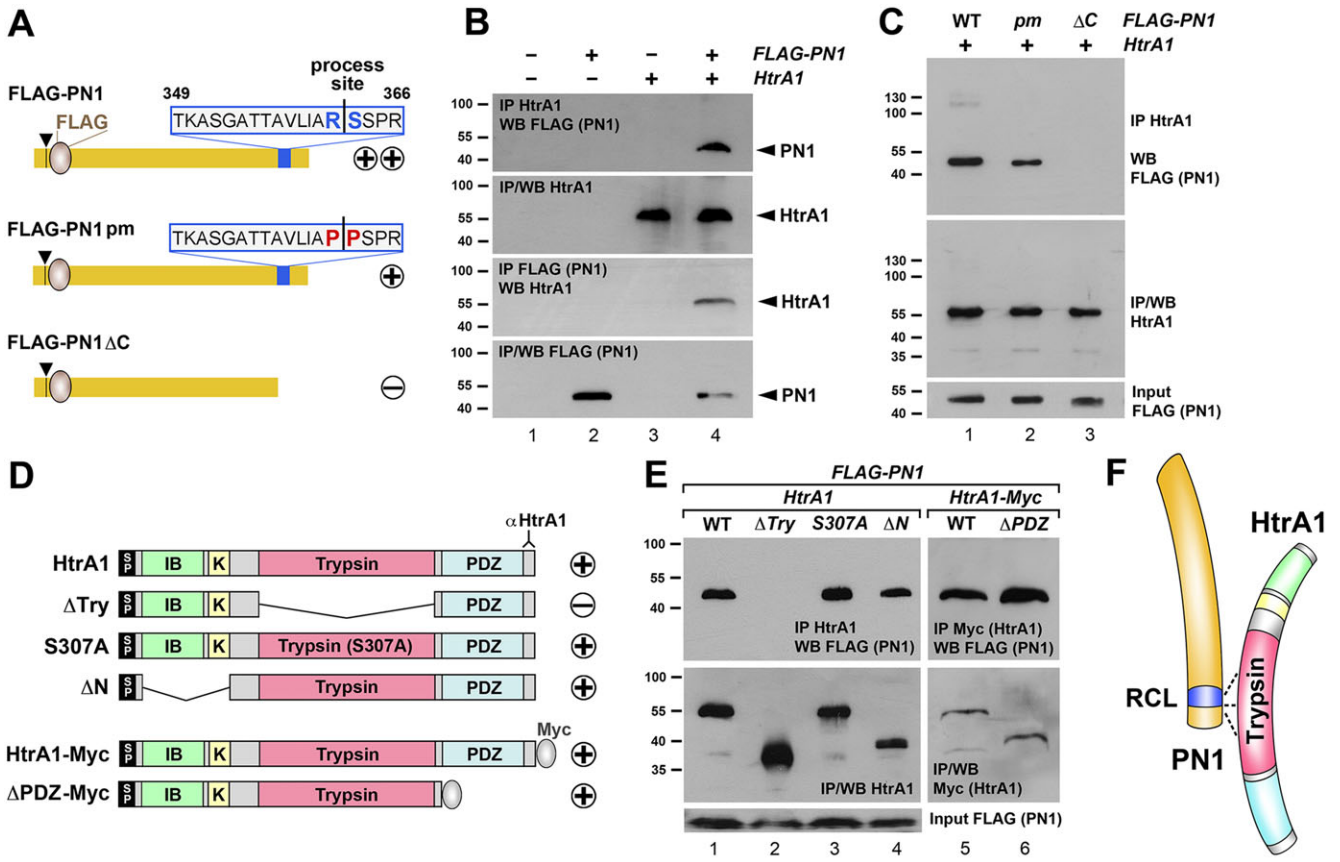

Fig. 3. PN1 binds to HtrA1. (A) Overview of FLAG-tagged protein constructs of wild-type PN1, point mutant PN1pm and C-terminal deletion mutant PN1ΔC. Arrowhead indicates the signal peptide cleavage site and numbers indicate the amino acid position of the reactive center loop (RCL). Plus/minus signs indicate binding to HtrA1 protein. (B) HtrA1 co-immunoprecipitates with FLAG-PN1, and FLAG-PN1 in turn co-immunoprecipitates with HtrA1 in mRNA-injected embryos at stage 17. (C) Overexpressed HtrA1 immunoprecipitates FLAG-PN1pm less efficiently than FLAG-PN1 and fails to immunoprecipitate FLAG-PN1ΔC in embryos at stage 10.5. (D) Overview of wild-type and mutant HtrA1 protein constructs. Plus/minus signs indicate binding to PN1 protein. SP, signal peptide; IB, IGF-binding domain; K, kazal-type serine protease inhibitor domain; Trypsin, trypsin-like serine protease domain; PDZ, PSD95/DLG1/ZO1 domain. The region recognized by HtrA1 antibody is indicated. (E) All indicated HtrA1 constructs, except HtrA1ΔTry, immunoprecipitate FLAG-PN1 at similar levels in embryos at stage 11. (F) Model of PN1-HtrA1 interaction. The trypsin domain of HtrA1 binds to the RCL-containing C-terminus of PN1. (B,C,E) mRNA amounts were: *HtrA1*-derived, 100 pg; *PN1*-derived, 300 pg.

results from inhibition of canonical Wnt signaling, e.g. by the secreted Wnt antagonist Dkk1 (supplementary material Fig. S3D,F) (Glinka et al., 1998). We now show that an antisense morpholino oligonucleotide (MO) against *HtrA1* (*HtrA1*-MO), *XFD* mRNA and *Dkk1* mRNA reduce *Papc* and posteriorly expand *Otx2* expression (Fig. 2Y-AA), indicating that inhibition of HtrA1 and FGF resembles the effect of Wnt antagonism and promotes head formation. *HtrA1* mRNA rescued *PN1*-induced suppression of mesodermal fate, reduction of neuronal differentiation and stimulation of anterior development (Fig. 2C,N, T,BB). *Fgf4* mRNA also compensated *PN1*-induced anteriorization (Fig. 2CC). Expression of pCS2-*Wnt3a* (referred to as *Wnt3a*-DNA) reverted the expansion of *Otx2* but, unlike *Fgf4*, failed to rescue reduction of *Papc* expression by *PN1* (Fig. 2DD). These results indicate that HtrA1 overexpression can rescue all PN1 activities and that PN1-induced anteriorization depends on FGF and, at least in part, on Wnt signals.

PN1 can bind to and block HtrA1

To determine whether PN1 and HtrA1 physically interact, we performed co-immunoprecipitation with proteins overexpressed in *Xenopus* embryos (Fig. 3). We generated FLAG-tagged constructs of PN1, PN1pm and the deletion mutant PN1ΔC, which lacks the C-terminal RCL and serpin signature motif (Fig. 3A; supplementary material Fig. S1) (Onuma et al., 2006). Immunoblot analysis revealed that FLAG-PN1 co-precipitated efficiently with HtrA1 and that HtrA1, in turn, co-precipitated with FLAG-PN1 (Fig. 3B). HtrA1 co-immunoprecipitated with FLAG-PN1pm less efficiently than with FLAG-PN1 and not at all with FLAG-PN1ΔC (Fig. 3C), suggesting that PN1 binds via its C-terminal RCL to HtrA1.

We next explored the protein domains of HtrA1 that interact with PN1, using a series of HtrA1 mutant constructs (Fig. 3D). FLAG-PN1 co-immunoprecipitated with HtrA1ΔN and HtrA1ΔPDZ-Myc to a similar degree as with wild-type HtrA1 and HtrA1-Myc (Fig. 3E, lanes 1, 4-6) but failed to immunoprecipitate with HtrA1ΔTry (Fig. 3E, lane 2). This suggested that the trypsin domain, but not the IGF-binding domain, kazal-type serine protease inhibitor domain or the PDZ domain, of HtrA1 is important for the binding to PN1. Since FLAG-PN1 co-immunoprecipitated with equal levels of HtrA1 (S307A) and HtrA1 (Fig. 3E, lanes 1 and 3), the catalytic serine residue in the active site of the enzyme is unlikely to undergo a covalent linkage with the RCL of PN1. Moreover, co-immunoprecipitated PN1 and HtrA1 were detectable in SDS-PAGE as individual proteins (45 kDa and 55 kDa, respectively)

Development (2015) 142, 1146-1158 doi:10.1242/dev.113886

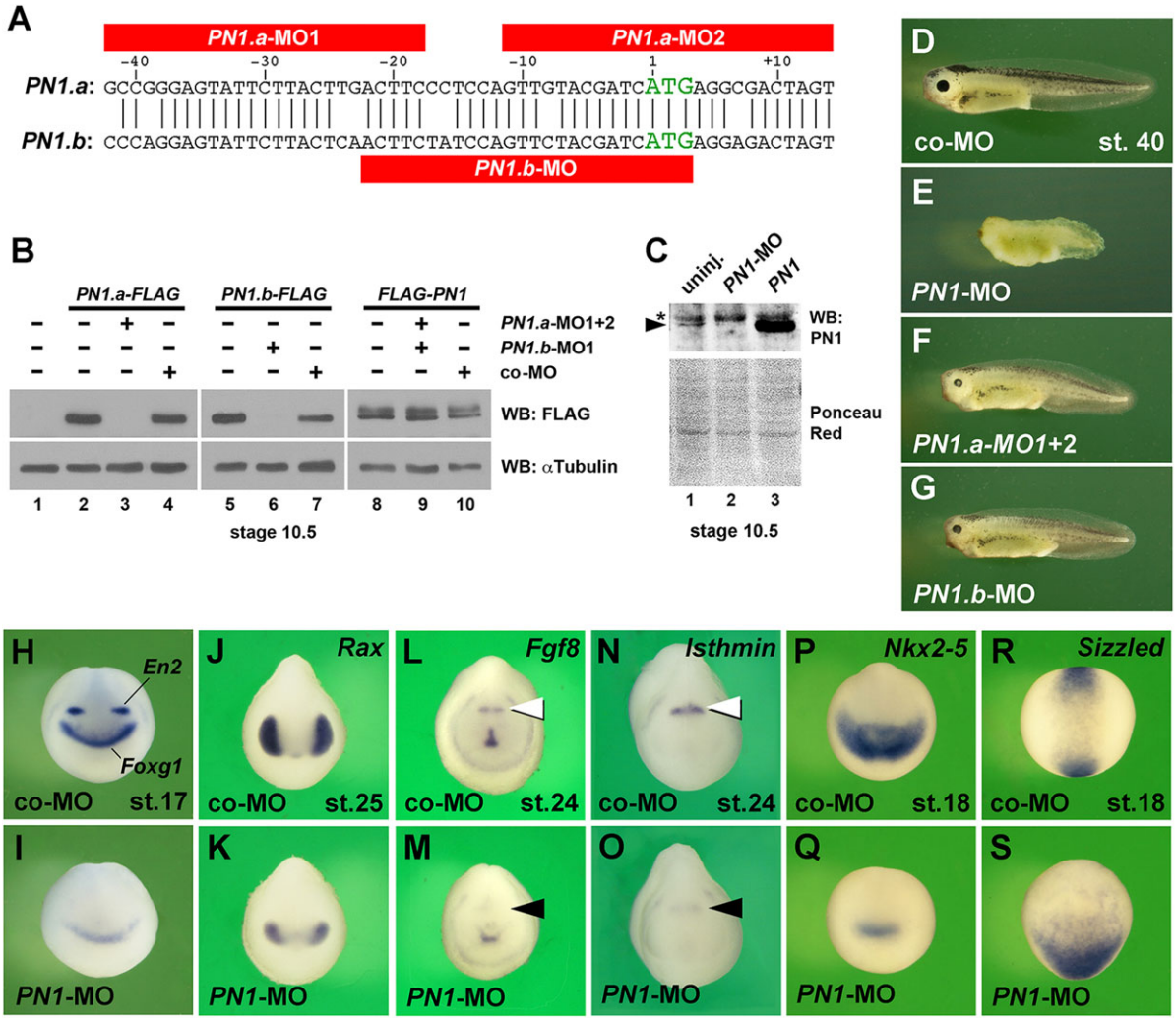

Fig. 4. Redundant functions of PN1.a and PN1.b in head and primary axis development. (A) Three antisense morpholino oligonucleotides (MOs) target the translation initiation sites of the *PN1.a* and *PN1.b* homeologs. (B) Immunoblot analysis of *Xenopus* gastrula embryos. *PN1.a*-MO1+2 and *PN1.b*-MO, but not standard control MO (co-MO), inhibit translation of injected *PN1.a-FLAG* and *PN1.b-FLAG* mRNAs (each 800 pg), respectively. Protein synthesis from non-targeted *FLAG-PN1* mRNA (800 pg) is not affected. WB, western blot. αTubulin provides a loading control. (C) *PN1*-MO blocks endogenous PN1 protein expression (arrowhead). The asterisk marks a non-specific band. Ponceau Red staining shows equal protein loading. (D) Co-MO-injected tadpole. (E-G) Microinjection of either *PN1.a*-MO1+2 or *PN1.b*-MO causes microcephaly. A combination of all three MOs (designated *PN1*-MO) results in severe reduction of head and shortening of tail structures. (H-Q) *PN1*-MO induces depletion of *En2* and reduction of *Foxg1*, *Rax* and *Nkx2-5* expression. *Fgf8* and *Ism* expression is severely reduced at the midbrain-hindbrain boundary (arrowheads). (R,S) Reduction of anterior and expansion of posterior *Sizzled* expression in *PN1*-depleted embryo. Indicated phenotypes were shown by: D, 29/31; E, 125/161; F, 102/134; G, 34/38; H, 71/77; I, 26/28; J, 45/45; K, 60/67; L, 40/45; M, 61/66; N, 16/18; O, 25/29; P, 40/40; Q, 25/25; R, 53/54; S, 33/39.

but not as an SDS-stable 1:1 complex that resists the boiling and reducing conditions, further supporting that PN1 and HtrA1 may interact through non-covalent binding. This differs from published records, which show that PN1 forms stable covalent bonds with target proteases (Baker et al., 1980; Stone et al., 1987; Knauer et al., 2000). Together, our data suggest a non-covalent serpin-serine protease complex, in which the C-terminal RCL of PN1 specifically binds to the trypsin domain of HtrA1 (Fig. 3F).

In mRNA-injected embryos, *FLAG-PN1* suppressed *HtrA1*-induced anencephaly and ectopic tail structures, mesoderm induction and neuronal differentiation, whereas *FLAG-PN1pm* had only little and *FLAG-PN1ΔC* no rescuing effect (supplementary material Fig. S4). Thus, the ability of PN1 to counteract HtrA1 activities (PN1>PN1pm>PN1ΔC) reflects the strength of their interaction and suggests that an intact RCL is required for PN1 to antagonize HtrA1.

The two *PN1* genes have redundant functions in head and axial development

We performed loss-of-function studies to further investigate the role of PN1 in the embryo (Fig. 4). We used two non-overlapping MO sequences that target the translation initiation site of the *PN1.a* gene (*PN1.a*-MO1+2) and one MO directed against the *PN1.b* gene (*PN1.b*-MO) (Fig. 4A). Immunoblot analysis showed that *PN1.a*-MO1+2 and *PN1.b*-MO robustly blocked protein biosynthesis of PN1.a-FLAG and PN1.b-FLAG, respectively, in mRNA-injected *Xenopus* embryos, whereas a non-specific standard control MO (designated co-MO) had no effect (Fig. 4B). By contrast, translation of a non-targeted *FLAG-PN1* mRNA was not reduced by *PN1.a*-MO1+2 nor *PN1.b*-MO, underscoring their specificity. Using a polyclonal antibody against PN1, we were able to demonstrate that a combination of *PN1.a*-MO1+2 and *PN1.b*-MO (collectively termed *PN1*-MO

Development (2015) 142, 1146-1158 doi:10.1242/dev.113886

hereafter) significantly reduced endogenous PN1 protein levels in *Xenopus* gastrula embryos (Fig. 4C, lanes 1 and 2). The endogenous PN1 protein from uninjected embryos ran at the same level as overexpressed PN1 protein from mRNA-injected siblings (Fig. 4C, lanes 1 and 3), validating the anti-PN1 antibody.

Animal injection of *PN1*-MO caused a slight delay of blastopore closure during gastrulation, severe microcephaly and enlargement of the proctodeum at tailbud stage, and loss of eye and shortening of tail structures in tadpole embryos (Fig. 4D,E and Fig. 5U,V; supplementary material Fig. S5). Individual knockdown of PN1.a (*PN1.a*-MO1+2) or PN1.b (*PN1.b*-MO) led to mild microcephaly (Fig. 4F,G). Analysis of molecular markers confirmed that targeting each homeolog alone has weaker effects (supplementary material Fig. S6) than their compound knockdown (Fig. 4I and Fig. 5B; supplementary material Fig. S7D), underscoring the redundant functions of the two *PN1* genes. These and the following phenotypes were specific, as the co-MO (Figs 4-7; supplementary material Figs S5,

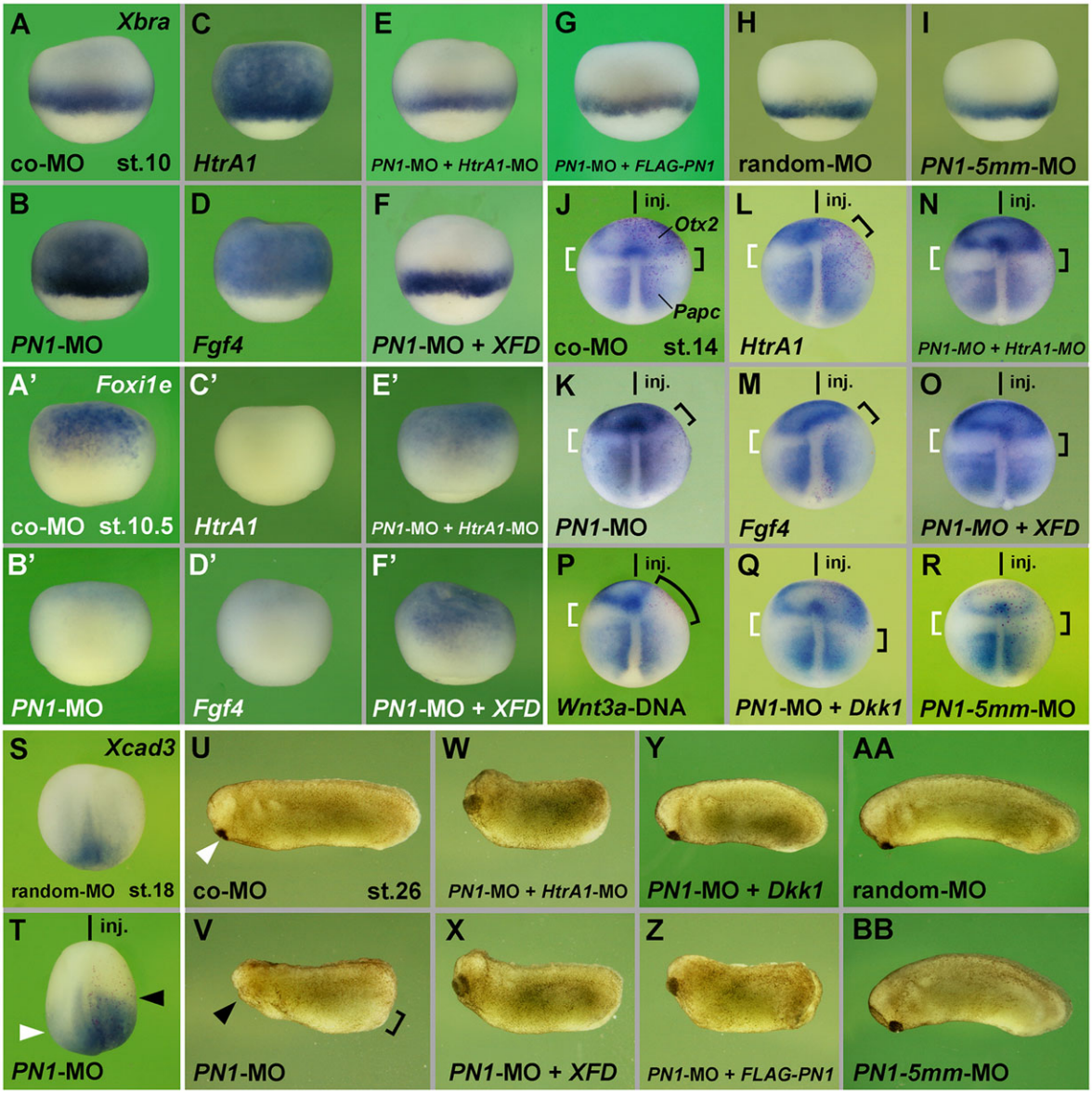

Fig. 5. PN1 functions in an HtrA1-, FGF- and Wnt-dependent manner. (A-D′) Lateral view of early gastrula embryos. *PN1*-MO, *HtrA1* mRNA and *Fgf4* mRNA, but not co-MO, induce ectopic *Xbra* expression (A-D) and a reduction of *Foxi1e* expression (A′-D′) in the animal hemisphere. (E-F′) In *PN1* morphant embryos, 20 ng *HtrA1*-MO and *XFD* mRNA restore normal expression of *Xbra* and *Foxi1e*. (G-I) Random-MO, *PN1-5mm*-MO, and a combination of *PN1*-MO and non-targeted *FLAG-PN1* mRNA do not affect *Xbra* expression. (J-T) Dorsal view of neurulae. A single injection of *PN1*-MO shifts the border between *Otx2* and *Papc* (brackets in K) and expands *Xcad3* expression (arrowheads in T) anteriorward. Co-MO and *PN1-5mm*-MO have no effect on *Otx2* and *Papc* (J,R), and random-MO has no effect on *Xcad3* expression (S). *HtrA1* mRNA, *Fgf4* mRNA and *Wnt3a*-DNA reduce *Otx2*, but only *HtrA1* and *Fgf4* expand *Papc* expression (L, M,P). Co-injections of 5 ng *HtrA1*-MO, *XFD* and *Dkk1* mRNA revert the effect of *PN1*-MO and cause slight expansion of *Otx2* and posteriorward retraction of *Papc* signals (N,O,Q). (U-BB) *PN1*-MO reduces head structures (arrowhead) and expands the proctodeum (bracket in V), whereas co-MO, random-MO and *PN1-5mm*-MO have no effect in tailbud embryos (U,AA,BB). 20 ng *HtrA1*-MO, *XFD*, *Dkk1* and *FLAG-PN1* rescue posteriorization in *PN1* morphants (W-Z). Injected mRNA amounts per embryo were: *HtrA1*, 200 pg (50 pg in L); *Fgf4*, 2 pg (0.5 pg in M); *XFD*, 80 pg (20 pg in O); *FLAG-PN1*, 800 pg; *Dkk1*, 24 pg (8 pg in Q). Indicated phenotypes were shown by: A, 136/144; A′, 50/59; B, 154/186; B′, 50/69; C, 21/21; C′, 47/57; D, 79/79; D′, 93/97; E, 66/90; E′, 52/56; F, 72/83; F′, 45/51; G, 24/30; H, 44/46; I, 14/24; J, 12/13; K, 14/14; L, 60/60; M, 45/49; N, 17/17; O, 9/9; P, 34/36; Q, 55/55; R, 31/32; S, 8/8; T, 28/30; U, 75/77; V, 97/95; W, 48/59; X, 23/24; Y, 67/65; Z, 22/23; AA, 7/10; BB, 10/15.

Development (2015) 142, 1146-1158 doi:10.1242/dev.113886

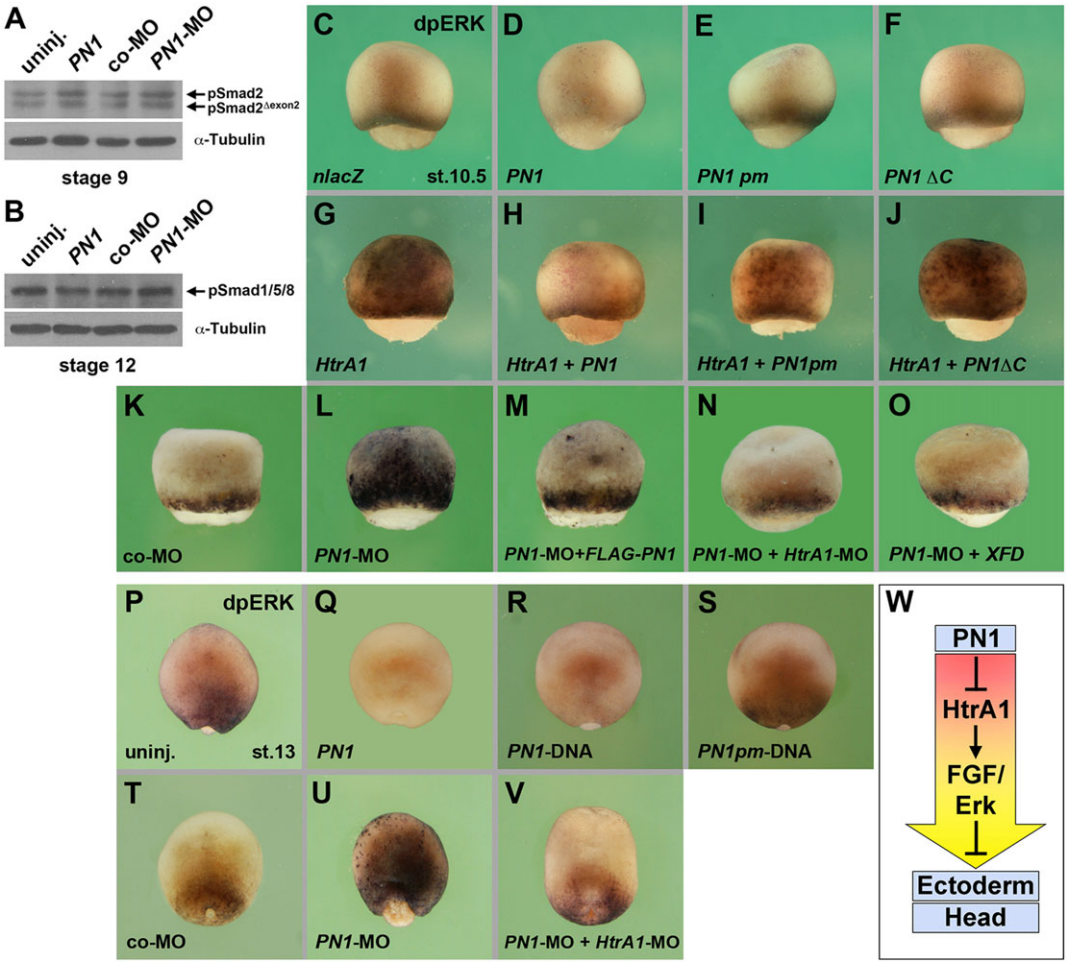

Fig. 6. PN1 specifically blocks FGF/Erk signaling via inhibition of HtrA1. (A,B) Immunoblot analysis of *Xenopus* embryos. Injection of *PN1* mRNA, co-MO or *PN1*-MO has no effect on phosphorylated Smad2 (pSmad2/pSmad2Δexon2) at stage 9 nor on pSmad1/5/8 at stage 12. *Xenopus* Smad proteins run between 55 and 60 kDa (Faure et al., 2000). (C-F) Early gastrula embryos in lateral view after immunostaining for activated Erk (dpERK). A single marginal injection of *PN1*, but not *PN1pm* or *PN1ΔC* mRNA, inhibits endogenous Erk phosphorylation in the marginal zone. (G-J) A single animal injection of *HtrA1* mRNA induces ectopic dpERK signals in the animal cap. *PN1* blocks *HtrA1*-induced Erk activation. *PN1pm* has weak and *PN1ΔC* has no rescuing effect. (K-O) *PN1*-MO, but not co-MO, induces ectopic dpERK in the animal hemisphere. Co-injection of non-targeted *FLAG-PN1* mRNA, 20 ng *HtrA1*-MO and *XFD* mRNA restores normal Erk activation in *PN1* morphant embryos. (P-V) Dorsal view of late gastrula embryos. Injections of *PN1* mRNA and pCS2-*PN1* (*PN1*-DNA), but not pCS2-*PN1pm* (*PN1pm*-DNA), suppress dpERK signals in the posterior mesoderm (Q-S). *PN1*-MO induces anteriorward expansion of active Erk (U), which is reverted by co-injection of *HtrA1*-MO (V). (W) Deduced model of PN1 action. PN1 stimulates ectoderm and head development by inhibition of HtrA1 and FGF/Erk signaling. Injected mRNA amounts were: *PN1*-derived, 4 ng (800 pg in C-F,K-O; 300 pg in G-J); *HtrA1*, 100 pg; *XFD*, 80 pg. Indicated phenotypes were shown by: C, 23/25; D, 37/49; E, 17/22; F, 25/31; G, 86/93; H, 79/90; I, 40/45; J, 57/74; K, 92/96; L, 122/139; M, 25/35; N, 25/28; O, 17/19; P, 73/73; Q, 7/7; R, 23/33; S, 20/21; T, 43/46; U, 9/12; V, 39/47.

S7-S10), a random-MO (Fig. 5H,S,AA) and a *PN1-5mm*-MO, which contains five base mismatches with the *PN1.a* and *PN1.b* target mRNAs (Fig. 5I,R,BB), had no effect, and the effects of the *PN1*-MO were reverted by co-injection of non-targeted *FLAG-PN1* mRNA (Fig. 5G,Z and Fig. 6M).

PN1 morphant embryos showed depletion of *En2* and reduction of *Foxg1*, *Rax*, *Fgf8* and *Isthmin* expression at the boundary between mid and hindbrain (Fig. 4H-O). Injected *PN1*-MO also reduced *Nkx2-5* and *Sizzled* expression in the anterior heart mesoderm, while *Sizzled* expression in the ventroposterior mesoderm was expanded (Fig. 4P-S). These findings suggest an important role of PN1 in promoting anterior development.

PN1 activity depends on HtrA1, FGF and zygotic Wnt signals

We further investigated germ layer formation and anteroposterior axis development in PN1-depleted embryos (Fig. 5). Excessive mesoderm formation and posteriorization have previously been reported for overexpression of HtrA1 (Hou et al., 2007) and Fgf4 (Isaacs et al., 1994). At the early gastrula stage, animally injected *PN1*-MO, *HtrA1* mRNA and *Fgf4* mRNA caused ectopic *Xbra* expression and reduction of ectodermal *Foxi1e* expression in the animal hemisphere (Fig. 5A-D′). More careful analysis of hemisections revealed that the expansion of *Xbra* and concomitant loss of *Foxi1e* expression in response to *PN1*-MO, *HtrA1* and *Fgf4* are restricted to deep cells, while the outer layer of the animal cap never showed ectopic *Xbra* signals (supplementary material Fig. S8A-D′). To test whether the mesoderm expansion in PN1-depleted embryos was due to elevated HtrA1 and FGF receptor activities, we removed the function of this protease and of FGFR1 in the *PN1* morphant background. Animal injection of both *HtrA1*-MO and *XFD* mRNA restored the normal distribution of *Xbra* and rescued *Foxi1e* expression in *PN1* morphant embryos (Fig. 5E-F′; supplementary material Fig. S8E-F′), suggesting that PN1 promotes ectoderm and suppresses mesoderm in an HtrA1- and FGF-dependent manner.

Development (2015) 142, 1146-1158 doi:10.1242/dev.113886

At the neurula stage, *PN1*-MO reduced *Otx2* and expanded *Papc* and *Xcad3* expression anteriorly (Fig. 5K,T; supplementary material Fig. S7C,D). In comparison, both *HtrA1* and *Fgf4* mRNAs translocated the border between *Otx2* and *Papc* expression anteriorward (Fig. 5L,M). Sectioned embryos revealed that the mesodermal marker *Papc* did not spread to the overlying ectoderm upon *PN1*-MO, *HtrA1* mRNA and *Fgf4* mRNA injection (supplementary material Fig. S9). *Wnt3a*-DNA robustly reduced *Otx2* (Min et al., 2011), but did not anteriorly expand *Papc* expression (Fig. 5P). *HtrA1*-MO, *XFD* mRNA, the dominant negative FGF receptor-4a mRNA *dXFGFR4a* (Hongo et al., 1999) and *Dkk1* mRNA reverted *PN1*-MO-induced posteriorization (Fig. 5N,O,Q; supplementary material Fig. S7E,F) and restored head structures in *PN1* morphant tailbud embryos (Fig. 5W,Y), underscoring the need not only to inhibit Wnt, but also to suppress HtrA1 and FGF receptor activities in head formation. Together, our data suggest that the function of PN1 to promote anterior head development relies on endogenous HtrA1, FGF and zygotic Wnt signaling.

PN1 specifically regulates FGF/Erk signaling through inhibition of HtrA1

Since TGFβ/Nodal signals promote mesoderm induction (Kimelman, 2006) and BMP and maternal Wnt signals promote dorsoventral development (De Robertis et al., 2000; Niehrs, 2004), we asked whether PN1 affects these pathways. Smad2 and Smad1/5/8 are specific signal transducers of Nodal and BMP signals, respectively (Faure et al., 2000). Immunoblot analysis of injected *Xenopus* embryos showed that neither *PN1* mRNA nor *PN1*-MO induced any changes in the C-terminal phosphorylation of Smad2 at blastula stage (Fig. 6A) and of Smad1/5/8 at gastrula stage (Fig. 6B). The failure of PN1 to misregulate the expression of *Sox17a* (a Nodal target; Hudson et al., 1997), *Vent2* (a BMP target; Hata et al., 2000), *Gsc* (a Nodal and Wnt target; Watabe et al., 1995) and *Xnr3* (a Wnt target; McKendry et al., 1997) in gain- and loss-of-function experiments (supplementary material Fig. S10) further supports the notion that PN1 does not affect early signaling by members of the TGFβ family or maternal Wnt signals during dorsoventral patterning. The observation that PN1 inhibits transcription of *Xbra* (Fig. 2N and Fig. 5B) and *Xcad3* (Fig. 5T), which are immediate early targets of the FGF pathway (Latinkic et al., 1997; Isaacs et al., 1998), underscores that PN1 may antagonize FGF signals.

To validate that PN1 regulates FGF signaling, we used the doubly phosphorylated form of Erk (dpERK) as specific readout of FGF signaling (Christen and Slack, 1999). Immunohistochemical analysis of early gastrula embryos showed that *PN1* mRNA, but neither *PN1pm* nor *PN1ΔC*, blocked endogenous Erk activation in the marginal zone (Fig. 6C-F). *HtrA1* mRNA-induced expansion of dpERK into the animal hemisphere (Fig. 6G) (Hou et al., 2007) was blocked by co-injection of *PN1* mRNA, less by *PN1pm* and not at all by *PN1ΔC* (Fig. 6H-J). *PN1*-MO induced animalward expansion of dpERK signals, an effect that was reverted by *HtrA1*-MO and *XFD* mRNA (Fig. 6K,L,N,O), further demonstrating that PN1 restricts Erk activation in the ectoderm through inhibiting HtrA1 and FGF receptor signaling. At the late gastrula stage, robust dpERK signals were observed in the posterior mesoderm (Fig. 6P) (Christen and Slack, 1999). Injected *PN1* mRNA and pCS2-*PN1* (referred to as *PN1*-DNA), which is expressed only after the midblastula transition, blocked posterior Erk activation, whereas pCS2-*PN1pm* (*PN1pm*-DNA) had no effect (Fig. 6Q-S). By contrast, *PN1*-MO expanded dpERK signals towards the anterior pole (Fig. 6T,U), and co-injected *HtrA1*-MO reverted this phenotype (Fig. 6V), suggesting that PN1 protects the anterior territory of the embryo against posteriorizing FGF/Erk signals via inhibition of HtrA1. We conclude that PN1 promotes ectoderm and head development by antagonizing HtrA1 and FGF/Erk signaling (Fig. 6W).

PN1 regulates paracrine signaling and diffusion of FGFs

We previously introduced an animal cap sandwich assay to demonstrate that HtrA1 stimulates the long-range distribution of FGF signals in the extracellular space (Hou et al., 2007). Here, we investigate the impact of PN1 on FGF paracrine signaling (Fig. 7A-K). An inducer animal cap injected with *nlacZ* mRNA as a lineage tracer was recombined with a responder cap. Following 6 h culture, the sandwiches were stained with X-Gal and analyzed by *in situ* hybridization for expression of the FGF target *Xbra* (Fig. 7A). An *Fgf4* and *HtrA1* mRNA-injected inducer cap caused robust elongation and widespread *Xbra* expression in the adjacent responder cap (Fig. 7B,C) (Hou et al., 2007). Concomitant overexpression of *PN1*, but not *PN1pm*, blocked the effects by *HtrA1* and *Fgf4* (Fig. 7D,E). Whereas co-MO and *PN1*-MO injection alone had no effect (Fig. 7F, G), a combination of *Fgf4* mRNA and co-MO triggered moderate elongation and *Xbra* signals close to the interface with the injected inducer cap (Fig. 7H). Notably, *Fgf4* mRNA and *PN1*-MO caused pronounced elongation of the uninjected responder cap and robust *Xbra* expression even at distance from the Fgf4 source (Fig. 7I). The presented data are statistically significant (Fig. 7J,K) and suggest an essential role of PN1 in regulating FGF paracrine signaling.

Christen and Slack (1999) reported an elegant experiment to analyze the spread of FGF proteins in *Xenopus* embryos. Following injection of digoxigenin (DIG)-labeled *Fgf4* mRNA into one animal blastomere at the 32-cell stage, a ring of dpERK-positive cells is induced in the animal cap around the exogenous FGF source after the midblastula transition (Fig. 7L). It was previously shown that this Erk activation outside of the source area is due to diffusion of FGF proteins (Christian and Slack, 1999). At stage 8.5, ectopic Erk activation spanned about one cell diameter around the *Fgf4* mRNA injection site (Fig. 7M). Upon co-injection of *Fgf4* and *HtrA1* mRNAs, signals spread approximately eight cell diameters from the source (Fig. 7N). This eightfold increase in diameter (a 64-fold increase in area) of the activated dpERK patch indicated that HtrA1 facilitates FGF diffusion. HtrA1-mediated expansion of Erk activation was strongly reduced by co-injection of *PN1* mRNA, but only a little by *PN1pm* mRNA (Fig. 7O,P). By contrast, microinjection of *PN1*-MO augmented the diameter of *Fgf4*-induced Erk activation almost threefold compared with co-MO (Fig. 7Q,R). Co-injection of *HtrA1*-MO limited the spread of Erk signals in *PN1* morphant embryos (Fig. 7S), suggesting that PN1 functions to restrict FGF diffusion in an HtrA1-dependent manner. The observation that co-injection of *XFD* mRNA completely blocked *Fgf4*-induced dpERK expression in PN1-deficient embryos (Fig. 7T) confirms that FGF signals account for the expansion of Erk activation. A quantification of the data is presented in Fig. 7U and suggests a key role for PN1 in regulating FGF diffusion.

PN1 stabilizes Sdc4 against degradation by HtrA1

In *Xenopus*, the transmembrane proteoglycan Sdc4 is co-expressed with PN1 in the early animal hemisphere of blastula and anterior neural plate of neurula embryos (Muñoz et al., 2006; Kuriyama and Mayor, 2009). Moreover, Sdc4 is a proteolytic target of HtrA1 (Hou et al., 2007). Overexpression of *HA-PN1* increased protein levels of FLAG-Sdc4 (Fig. 7V, lanes 2 and 3) and reverted *HtrA1*-induced breakdown of FLAG-Sdc4 proteins (Fig. 7V, lanes 4 and 5). By contrast, *PN1*-MO reduced protein levels of FLAG-Sdc4 (Fig. 7W). The results suggest that PN1 might stabilize Sdc4 in the embryo and protect this proteoglycan from degradation by the HtrA1 protease.

Development (2015) 142, 1146-1158 doi:10.1242/dev.113886

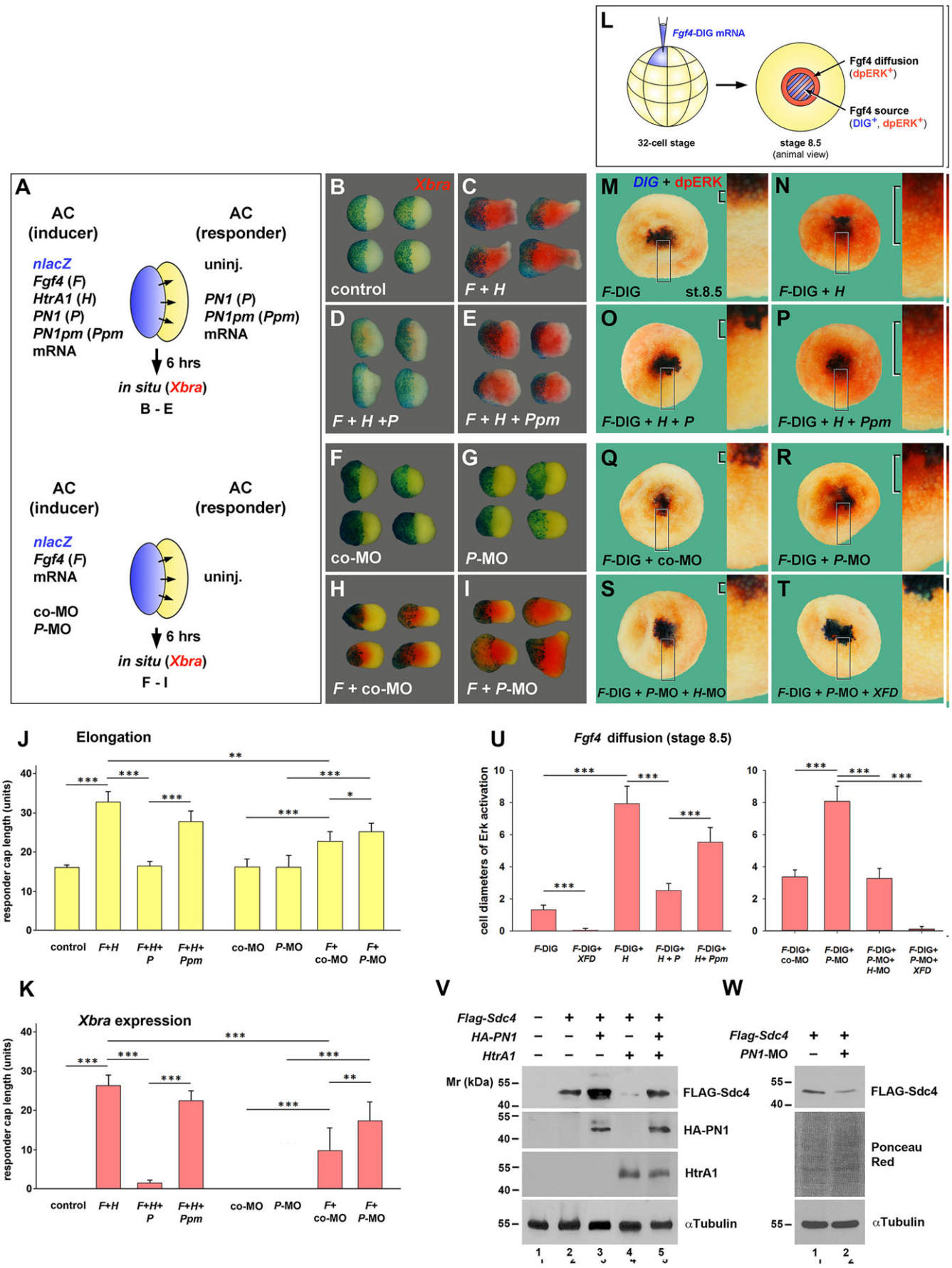

Fig. 7. See the next page for legend.

Development (2015) 142, 1146-1158 doi:10.1242/dev.113886

Fig. 7. PN1 regulates paracrine FGF signaling and the proteolytic cleavage of *Xenopus* Sdc4. (A) Experimental design of animal cap (AC) assay. (B) Control animal cap conjugates with *nlacZ* mRNA-injected inducer cap (blue) and uninjected responder cap remain round and do not express *Xbra*. (C-E) Injection of *Fgf4* and *HtrA1* mRNAs in the inducer cap triggers robust elongation and strong *Xbra* expression (red) in the responder cap, which is blocked by *PN1* but not *PN1pm* mRNA in the conjugate. (F,G) co-MO and *PN1*-MO alone do not trigger elongation nor *Xbra* expression. (H) *Fgf4* and co-MO in the inducer cap cause moderate elongation and low *Xbra* expression in the uninjected responder cap. (I) *Fgf4* and *PN1*-MO induce strong elongation and high levels of *Xbra* expression far from the signaling source. (J,K) Quantification of the elongation and extent of *Xbra* expression in the responder caps of injected animal cap sandwiches. (L) Experimental design of the Fgf4 diffusion assay. (M) Animal view of blastula embryo at stage 8.5 after double staining for *Fgf4*-DIG (blue) and dpERK (red). The inset to the right is a magnification of the framed area. Following injection of *Fgf4*-DIG mRNA into a single blastomere at the 32-cell stage, the Fgf4 signal spreads and activates Erk over about one cell diameter (bracket) outside of the injected area. (N) *HtrA1* further expands the Fgf4 signal and activates Erk about eight cell diameters away from the source. (O,P) *PN1*, but not *PN1pm*, restricts the *HtrA1*-triggered spread of the Fgf4/Erk signal. (Q,R) *PN1*-MO, but not co-MO, stimulates the spread of the Fgf4 signal. (S,T) In *PN1* morphant embryos, 20 ng *HtrA1*-MO and *XFD* mRNA limit the spread of the Fgf4 signal and reduce Erk activation. (U) Quantification of Fgf4 diffusion based on Erk activation in the animal hemisphere of injected blastula embryos. (V,W) Immunoblot of *Xenopus* embryos at stage 26 (V) and stage 14 (W). Note that *HA-PN1* stabilizes FLAG-Sdc4 protein and protects it against HtrA1-mediated degradation. Downregulation of PN1 lowers FLAG-Sdc4 protein amounts. The doses of injected mRNAs were: *Fgf4*, 60 pg; *FLAG-Sdc4*, 220 pg; *HtrA1*, 320 pg (160 pg in N-P, 80 pg in V); *nlacZ*, 200 pg; *PN1*-derived, 1200 pg (300 pg in O,P); *XFD*, 80 pg; *Fgf4-DIG*, 300 pg. Indicated phenotypes were shown by: B, 24/24; C, 25/25; D, 24/24; E, 24/24; F, 11/11; G, 12/12; H, 13/15; I, 9/10; M, 25/25; N, 14/14; O, 17/17; P, 11/11; Q, 22/22; R, 26/28; S, 17/18; T, 19/19. Data are expressed as mean±s.d. Statistical significance was determined using one-way ANOVA followed by unpaired Student's *t*-test. **P*<0.05, ***P*<0.01, ****P*<0.001.

DISCUSSION

In this study, we identified PN1 as an important feedback regulator of FGF signaling during ectoderm formation and head development. The finding that the transcription of two *Xenopus PN1* homeologs is positively regulated by FGF signals is consistent with previous reports that FGF2 stimulates murine *PN1* expression in primary mid/hindbrain and cultured cerebellum cells (Küry et al., 1997; Vaillant et al., 2007), supporting the contention that *PN1* might be an FGF target gene. PN1 is a member of the serpin family of serine protease inhibitors, with an RCL that participates in an unusual non-covalent binding to the proteolytic trypsin domain of HtrA1. PN1 blocks the activity of HtrA1 and prevents it from degrading the proteoglycan Sdc4. We show that PN1, via inhibition of HtrA1, regulates FGF diffusion and paracrine signaling in the early embryo.

Our functional study of PN1 and its link to the HtrA1-FGF axis reinforce the conclusion that germ layer formation and anteroposterior axis development are interrelated processes that share common molecular principles (Fig. 8A,B). In the early *Xenopus* gastrula, FGF/Erk signals and the transcription factor Xbra mutually activate each other (Isaacs et al., 1994; Schulte-Merker and Smith, 1995), and HtrA1 stimulates FGF/Erk signaling in the marginal zone (Hou et al., 2007), causing an expansion of mesoderm at the expense of ectoderm in the inner layer of the animal cap. We suggest that the animalward spread of mesodermal fate is blocked by FGF-activated PN1, which, through direct binding, inhibits HtrA1 and thereby restricts mesodermalizing FGF/Erk signaling (Fig. 8A). In support of this model, overexpression of PN1 blocks endogenous dpERK and *Xbra* expression in the marginal zone. An intact RCL domain is crucial for PN1 to inhibit HtrA1-induced Erk activation and mesoderm formation in the animal hemisphere. By contrast, downregulation of PN1 induces ectopic *Xbra* and reduction of ectodermal *Foxi1e* expression in deep cells of the animal cap, which could be the result of a morphogenetic movement defect or direct cell fate change. The observation that ectopic Erk activation and expansion of mesoderm at the expense of ectoderm cells in *PN1* morphant gastrula embryos can be reverted by both *HtrA1*-MO and *XFD* mRNA provides evidence that PN1 protects ectoderm and suppresses mesoderm via inhibition of HtrA1 and FGF/Erk signals.

At the early neurula stage, two fields have segregated along the primary body axis, with the anterior neural plate showing colocalization of PN1 and HtrA1 and the posterior mesoderm exhibiting an autocatalytic feedback of HtrA1, FGF/Erk and Xbra (Fig. 8B). PN1 blocks HtrA1 in the anterior domain and restricts HtrA1-FGF/Erk-Xbra activity to the posterior part of the embryo. In support of this conclusion, PN1 overexpression expands anterior at the expense of posterior marker genes in an HtrA1- and FGF-dependent manner, and zygotic PN1 suppresses posterior Erk activation, whereas PN1 knockdown has the opposite effect and expands expression of the FGF-responsive *Xcad3* gene. Previous studies have highlighted roles of FGF signals (Amaya et al., 1991) and HtrA1 (Hou et al., 2007) in posterior trunk/tail formation, but whether their activities need to be suppressed to allow head development has not conclusively been demonstrated. Here, we show that both *XFD* mRNA and *HtrA1*-MO expand the anterior ectoderm marker *Otx2* at the expense of the posterior mesoderm marker *Papc*. Moreover, the anteriorward expansion of Erk activation and reduction of anterior *Otx2* expression in PN1-depleted embryos is reverted by downregulation of FGF receptor and HtrA1 activities. Thus, FGF/Erk needs to be inhibited to allow head formation, and PN1 protects the head from this posteriorizing signaling. Taken together, PN1 is an antagonist of the HtrA1-FGF axis and fulfills important functions to maintain the ectoderm and head as default states.

We suggest a scenario in which PN1 controls long-range FGF signaling by regulating HtrA1-mediated cleavage of proteoglycans (Fig. 8C). Upon release from the cell, FGFs are bound by the HS chains of cell surface proteoglycans that restrict their diffusion (Yu et al., 2009). HS is abundant in the *Xenopus* blastula and neurula (Yamada et al., 2009). HtrA1 triggers cleavage of proteoglycans, including Sdc4 (Hou et al., 2007), and mobilizes FGFs complexed to its soluble ectodomain, thereby converting proteoglycans from negative diffusion regulators into shuttles that transport FGFs through the extracellular space. Notably, HS-bound FGFs are protected against degradation by secreted serine proteases (Saksela et al., 1988; Sommer and Rifkin, 1989). We show that, in the animal cap of stage 8.5 embryos, HtrA1 can expand the range of Erk activation up to eight cell diameters outside of an artificial Fgf4 source, suggesting that this protease is able to facilitate the diffusion of FGF proteins over a distance of 300 µm. As proteoglycans are important co-receptors of the FGF-FGFR signaling complex (Matsuo and Kimura-Yoshida, 2013), their unrestricted degradation might cause a collapse of FGF signaling. Moreover, HtrA1 can degrade free FGF8 protein (Kim et al., 2012), further underscoring the need to control HtrA1 proteolytic activity. PN1 binds to HS, which attracts the serpin to the cell surface and elevates protease inhibition (Li and Huntington, 2012). We showed that, through physical interaction, PN1 inhibits HtrA1 and stabilizes Sdc4. PN1 restricts HtrA1-stimulated FGF diffusion and fulfills a necessary function in controlling paracrine FGF/Erk signaling in the *Xenopus* embryo.

Development (2015) 142, 1146-1158 doi:10.1242/dev.113886

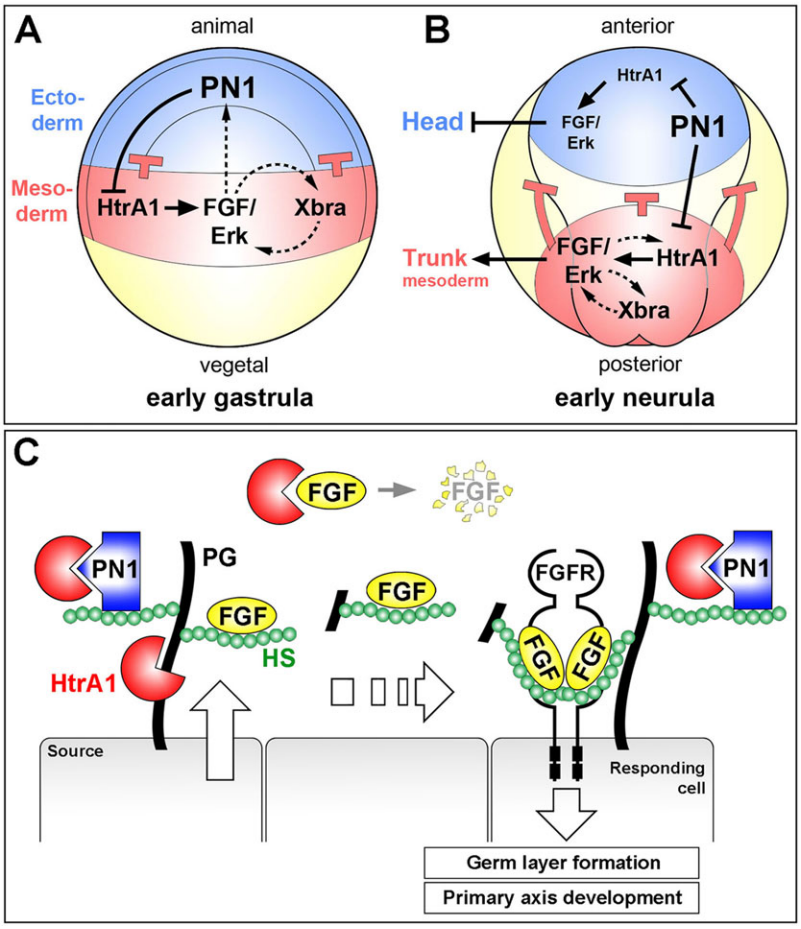

Fig. 8. Model for the spatial restriction of FGF signaling by PN1 in germ layer and primary axis development. (A,B) Feedback regulation of FGF/Erk signaling by the transcription factor Xbra and the secreted proteins HtrA1 and PN1 in early gastrula (lateral view, A) and early neurula (dorsal view, B) *Xenopus* embryo. Unbroken lines indicate biochemical interaction and dashed lines transcriptional regulation. Red bars represent inhibition of ectoderm and head development by mesodermal FGF signals. (C) Summary of the observations reported here and by Hou et al. (2007) of how the HtrA1 protease cleaves cell surface proteoglycans to mobilize FGF/proteoglycan messages that activate FGF receptors at a distance. As described by Kim et al. (2012), HtrA1 can also degrade non-bound FGF proteins. PN1, which binds to heparan sulfate (HS) (Li and Huntington, 2012), regulates paracrine FGF signaling by binding to and inhibiting HtrA1.

Proteoglycans via their HS chains bind to other growth factors in addition to FGFs, such as members of the TGFβ family, Wnts and Hh signals (Häcker et al., 2005). Yet in *Xenopus*, PN1 seems not to affect signaling intermediates and targets of the TGFβ pathways, nor target genes of the maternal Wnt/β-catenin pathway. Our findings that *Dkk1* overexpression rescues posteriorization in *PN1* morphant embryos, and that aspects of the anteriorizing effect of forced *PN1* expression can be compensated by *Wnt3a*-DNA, supports at least a partial involvement of zygotic Wnt signaling in PN1 action during primary axis development. A previous study indicated that the posteriorizing effect of FGF signaling can be indirectly mediated by Wnt, e.g. by secondary induction of *Wnt3a* or *Wnt8* (Kazanskaya et al., 2000). In addition, Sdc4 can positively regulate the Wnt/planar cell polarity pathway, which in turn inhibits Wnt/β-catenin signaling (Muñoz et al., 2006; Astudillo et al., 2014). Our observations that PN1 negatively regulates FGF signals and stabilizes Sdc4 protein in an HtrA1-dependent manner are consistent with a possible indirect inhibition of zygotic Wnt/β-catenin signaling by PN1. In mouse, PN1 inhibits Shh signaling in the postnatal cerebellum and in prostate cancer (Vaillant et al., 2007; McKee et al., 2012). However, Hh antagonism is unlikely to explain the PN1 activities described here because Hh signals do not induce mesoderm and – similar to PN1 – inhibit neuronal differentiation and promote anterior development in the early *Xenopus* embryo (Lai et al., 1995; Franco et al., 1999; Min et al., 2011).

Is the PN1-HtrA1-FGF interaction that we present here for germ layer and primary axis formation relevant for other aspects of development and disease? In the mouse postimplantation embryo, a crucial function of secreted serine proteases has recently been demonstrated for HSPG cleavage and spreading of Fgf4/8 proteins in the extra-embryonic ectoderm (Shimokawa et al., 2011). PN1 is expressed in the adjacent ectoplacental cone (Mansuy et al., 1993), suggesting a possible role for the local retention of FGF signals in these derivatives of the trophectoderm. Furthermore, HtrA1 is implicated in cancer, arthritis, age-related macular degeneration and Alzheimer's disease (Clausen et al., 2011). To our knowledge, PN1 is the first *in vivo* inhibitor of HtrA1 to be described. Thus, the functional interaction of PN1, HtrA1 and FGF signals, as established here for the *Xenopus* embryo, could be relevant for the formation of an early mammalian cell lineage and help to develop new therapies for human diseases.

MATERIALS AND METHODS

Constructs and microinjection

Unless indicated otherwise, MOs, mRNAs or DNAs were injected four times animally at the 2- or 4-cell stage. Co-MO, random-MO, *PN1-5mm*-MO, *PN1.a*-MO1+*PN1.a*-MO2 (30 ng each), *PN1.b*-MO or *PN1*-MO (20 ng each of *PN1.a*-MO1, *PN1.a*-MO2, *PN1.b*-MO) were injected at a total of 60 ng per embryo. For single injections with 100 pg *nlacZ* mRNA as lineage tracer, a quarter of the above indicated MO amounts were used. Injected amounts of DNA per embryo were: pCS2-*Wnt3a*, 30 pg; pCS2-*PN1*, 100 pg; pCS2-*PN1pm*, 100 pg. For MO sequences, details of *X. laevis PN1* and *HtrA1* expression constructs and mRNA preparation see the supplementary materials and methods and Table S1.

Embryo processing and expression analyses

Xenopus embryos and explants were prepared, cultured, microinjected and processed through Red-Gal staining, whole-mount *in situ* hybridization, and whole-mount immunostaining with anti-dpERK antibody (Cell Signaling

Technology, 9101; 1:250) as described (Pera et al., 2015). The preparation of DIG-labeled *Fgf4* RNA and double staining of DIG with NBT/BCIP (Roche) followed by dpERK with Fast Red (Roche) were performed according to Christen and Slack (1999). RT-PCR was performed as previously described (Hou et al., 2007) using the primers listed in supplementary material Table S2.

Xenopus PN1 antibody, immunoprecipitation and immunoblotting

A peptide of *X. laevis* PN1 (amino acids 198-212, PENTKKRTFHGPDGK-Cys) was synthesized and used as antigen to raise a polyclonal rabbit antibody (Proteogenix, Oberhausbergen, France). Details of immunoprecipitation and immunoblotting are provided in the supplementary materials and methods.

Acknowledgements

We thank E. Amaya, I. Dawid, E. De Robertis, R. Harland, H. Isaacs, C. Niehrs, J. Slack, D. Weinstein, A. Zaraisky and J. Larrain for plasmids, and O. Wessely and U. Häcker for critical review of the manuscript.

Competing interests

The authors declare no competing or financial interests.

Author contributions

H.A., D.I., T.H.M.G., M.M. and E.M.P. designed experiments, performed research and analyzed data. N.G., J.G., S.H. and M.S. performed research. M.C. performed statistical analysis. E.M.P. wrote the manuscript.

Funding

This work was funded by grants from the Swedish Research Council [2006-5286 and 2009-4951 to E.M.P.], the Swedish Child Cancer Foundation [PROJ09/124 and PROJ11/101 to E.M.P.; NBCNSPDHEL12/02 to N.G.] and the Crafoord Foundation. M.M. receives funds from the Swedish Cancer foundation [CAN2013/625 to M.M.]. S.H. and J.G. were Erasmus Fellows.

Supplementary material

Supplementary material available online at
http://dev.biologists.org/lookup/suppl/doi:10.1242/dev.113886/-/DC1

References

Amaya, E., Musci, T. J. and Kirschner, M. W. (1991). Expression of a dominant negative mutant of the FGF receptor disrupts mesoderm formation in Xenopus embryos. *Cell* **66**, 257-270.

Astudillo, P., Carrasco, H. and Larraín, J. (2014). Syndecan-4 inhibits Wnt/β-catenin signaling through regulation of low-density-lipoprotein receptor-related protein (LRP6) and R-spondin 3. *Int. J. Biochem. Cell Biol.* **46**, 103-112.

Baker, J. B., Low, D. A., Simmer, R. L. and Cunningham, D. D. (1980). Protease-nexin: a cellular component that links thrombin and plasminogen activator and mediates their binding to cells. *Cell* **21**, 37-45.

Böttcher, R. T. and Niehrs, C. (2005). Fibroblast growth factor signaling during early vertebrate development. *Endocr. Rev.* **26**, 63-77.

Christen, B. and Slack, J. M. (1999). Spatial response to fibroblast growth factor signalling in Xenopus embryos. *Development* **126**, 119-125.

Clausen, T., Kaiser, M., Huber, R. and Ehrmann, M. (2011). HTRA proteases: regulated proteolysis in protein quality control. *Nat. Rev. Mol. Cell Biol.* **12**, 152-162.

De Robertis, E. M., Larraín, J., Oelgeschläger, M. and Wessely, O. (2000). The establishment of Spemann's organizer and patterning of the vertebrate embryo. *Nat. Rev. Genet.* **1**, 171-181.

Faure, S., Lee, M. A., Keller, T., ten Dijke, P. and Whitman, M. (2000). Endogenous patterns of TGFbeta superfamily signaling during early Xenopus development. *Development* **127**, 2917-2931.

Ferrer-Vaquer, A., Maurey, P., Werzowa, J., Firnberg, N., Leibbrandt, A. and Neubüser, A. (2008). Expression and regulation of HTRA1 during chick and early mouse development. *Dev. Dyn.* **237**, 1893-1900.

Franco, P. G., Paganelli, A. R., López, S. L. and Carrasco, A. E. (1999). Functional association of retinoic acid and hedgehog signaling in Xenopus primary neurogenesis. *Development* **126**, 4257-4265.

Glinka, A., Wu, W., Delius, H., Monaghan, A. P., Blumenstock, C. and Niehrs, C. (1998). Dickkopf-1 is a member of a new family of secreted proteins and functions in head induction. *Nature* **391**, 357-362.

Häcker, U., Nybakken, K. and Perrimon, N. (2005). Heparan sulphate proteoglycans: the sweet side of development. *Nat. Rev. Mol. Cell Biol.* **6**, 530-541.

Hardcastle, Z., Chalmers, A. D. and Papalopulu, N. (2000). FGF-8 stimulates neuronal differentiation through FGFR-4a and interferes with mesoderm induction in Xenopus embryos. *Curr. Biol.* **10**, 1511-1514.

Hata, A., Seoane, J., Lagna, G., Montalvo, E., Hemmati-Brivanlou, A. and Massagué, J. (2000). OAZ uses distinct DNA- and protein-binding zinc fingers in separate BMP-Smad and Olf signaling pathways. *Cell* **100**, 229-240.

Hongo, I., Kengaku, M. and Okamoto, H. (1999). FGF signaling and the anterior neural induction in Xenopus. *Dev. Biol.* **216**, 561-581.

Hou, S., Maccarana, M., Min, T. H., Strate, I. and Pera, E. M. (2007). The secreted serine protease xHtrA1 stimulates long-range FGF signaling in the early Xenopus embryo. *Dev. Cell* **13**, 226-241.

Hudson, C., Clements, D., Friday, R. V., Stott, D. and Woodland, H. R. (1997). Xsox17alpha and -beta mediate endoderm formation in Xenopus. *Cell* **91**, 397-405.

Isaacs, H. V., Pownall, M. E. and Slack, J. M. (1994). eFGF regulates Xbra expression during Xenopus gastrulation. *EMBO J.* **13**, 4469-4481.

Isaacs, H. V., Pownall, M. E. and Slack, J. M. W. (1998). Regulation of Hox gene expression and posterior development by the Xenopus caudal homologue Xcad3. *EMBO J.* **17**, 3413-3427.

Kazanskaya, O., Glinka, A. and Niehrs, C. (2000). The role of Xenopus dickkopf1 in prechordal plate specification and neural patterning. *Development* **127**, 4981-4992.

Kim, G.-Y., Kim, H.-Y., Kim, H.-T., Moon, J.-M., Kim, C.-H., Kang, S. and Rhim, H. (2012). HtrA1 is a novel antagonist controlling fibroblast growth factor (FGF) signaling via cleavage of FGF8. *Mol. Cell. Biol.* **32**, 4482-4492.

Kimelman, D. (2006). Mesoderm induction: from caps to chips. *Nat. Rev. Genet.* **7**, 360-372.

Knauer, D. J., Majumdar, D., Fong, P.-C. and Knauer, M. F. (2000). SERPIN regulation of factor XIa. The novel observation that protease nexin 1 in the presence of heparin is a more potent inhibitor of factor XIa than C1 inhibitor. *J. Biol. Chem.* **275**, 37340-37346.

Kuriyama, S. and Mayor, R. (2009). A role for Syndecan-4 in neural induction involving ERK- and PKC-dependent pathways. *Development* **136**, 575-584.

Küry, P., Schaeren-Wiemers, N. and Monard, D. (1997). Protease nexin-1 is expressed at the mouse met-/mesencephalic junction and FGF signaling regulates its promoter activity in primary met-/mesencephalic cells. *Development* **124**, 1251-1262.

Lai, C. J., Ekker, S. C., Beachy, P. A. and Moon, R. T. (1995). Patterning of the neural ectoderm of Xenopus laevis by the amino-terminal product of hedgehog autoproteolytic cleavage. *Development* **121**, 2349-2360.

Latinkic, B. V., Umbhauer, M., Neal, K. A., Lerchner, W., Smith, J. C. and Cunliffe, V. (1997). The Xenopus Brachyury promoter is activated by FGF and low concentrations of activin and suppressed by high concentrations of activin and by paired-type homeodomain proteins. *Genes Dev.* **11**, 3265-3276.

Lea, R., Papalopulu, N., Amaya, E. and Dorey, K. (2009). Temporal and spatial expression of FGF ligands and receptors during Xenopus development. *Dev. Dyn.* **238**, 1467-1479.

Li, W. and Huntington, J. A. (2012). Crystal structures of protease nexin-1 in complex with heparin and thrombin suggest a 2-step recognition mechanism. *Blood* **120**, 459-467.

Mansuy, I. M., van der Putten, H., Schmid, P., Meins, M., Botteri, F. M. and Monard, D. (1993). Variable and multiple expression of Protease Nexin-1 during mouse organogenesis and nervous system development. *Development* **119**, 1119-1134.

Matsuo, I. and Kimura-Yoshida, C. (2013). Extracellular modulation of Fibroblast Growth Factor signaling through heparan sulfate proteoglycans in mammalian development. *Curr. Opin. Genet. Dev.* **23**, 399-407.

McKee, C. M., Xu, D., Cao, Y., Kabraji, S., Allen, D., Kersemans, V., Beech, J., Smart, S., Hamdy, F., Ishkanian, A. et al. (2012). Protease nexin 1 inhibits hedgehog signaling in prostate adenocarcinoma. *J. Clin. Invest.* **122**, 4025-4036.

McKendry, R., Hsu, S.-C., Harland, R. M. and Grosschedl, R. (1997). LEF-1/TCF proteins mediate wnt-inducible transcription from the Xenopus nodal-related 3 promoter. *Dev. Biol.* **192**, 420-431.

Min, T. H., Kriebel, M., Hou, S. and Pera, E. M. (2011). The dual regulator Sufu integrates Hedgehog and Wnt signals in the early Xenopus embryo. *Dev. Biol.* **358**, 262-276.

Muñoz, R., Moreno, M., Oliva, C., Orbenes, C. and Larraín, J. (2006). Syndecan-4 regulates non-canonical Wnt signalling and is essential for convergent and extension movements in Xenopus embryos. *Nat. Cell Biol.* **8**, 492-500.

Niehrs, C. (2004). Regionally specific induction by the Spemann-Mangold organizer. *Nat. Rev. Genet.* **5**, 425-434.

Olson, S. T. and Gettins, P. G. W. (2011). Regulation of proteases by protein inhibitors of the serpin superfamily. *Prog. Mol. Biol. Transl. Sci.* **99**, 185-240.

Onuma, Y., Asashima, M. and Whitman, M. (2006). A Serpin family gene, Protease nexin-1 has an activity distinct from protease inhibition in early Xenopus embryos. *Mech. Dev.* **123**, 463-471.

Development (2015) 142, 1146-1158 doi:10.1242/dev.113886

Pera, E. M., Hou, S., Strate, I., Wessely, O. and De Robertis, E. M. (2005). Exploration of the extracellular space by a large-scale secretion screen in the early Xenopus embryo. *Int. J. Dev. Biol.* **49**, 781-796.

Pera, E. M., Acosta, H., Gouignard, N., Climent, M. and Arregi, I. (2014). Active signals, gradient formation and regional specificity in neural induction. *Exp. Cell Res.* **321**, 25-31.

Pera, E. M., Acosta, H., Gouignard, N. and Climent, M. (2015). Whole-mount in situ hybridization and immunohistochemistry in Xenopus embryos. In *In Situ Hybridization Methods* (ed. G. Hauptmann). Springer (in press).

Saksela, O., Moscatelli, D., Sommer, A. and Rifkin, D. B. (1988). Endothelial cell-derived heparan sulfate binds basic fibroblast growth factor and protects it from proteolytic degradation. *J. Cell Biol.* **107**, 743-751.

Schulte-Merker, S. and Smith, J. C. (1995). Mesoderm formation in response to Brachyury requires FGF signalling. *Curr. Biol.* **5**, 62-67.

Shimokawa, K., Kimura-Yoshida, C., Nagai, N., Mukai, K., Matsubara, K., Watanabe, H., Matsuda, Y., Mochida, K. and Matsuo, I. (2011). Cell surface heparan sulfate chains regulate local reception of FGF signaling in the mouse embryo. *Dev. Cell* **21**, 257-272.

Sommer, A. and Rifkin, D. B. (1989). Interaction of heparin with human basic fibroblast growth factor: protection of the angiogenic protein from proteolytic degradation by a glycosaminoglycan. *J. Cell. Physiol.* **138**, 215-220.

Stone, S. R., Nick, H., Hofsteenge, J. and Monard, D. (1987). Glial-derived neurite-promoting factor is a slow-binding inhibitor of trypsin, thrombin, and urokinase. *Arch. Biochem. Biophys.* **252**, 237-244.

Umbhauer, M., Marshall, C. J., Mason, C. S., Old, R. W. and Smith, J. C. (1995). Mesoderm induction in Xenopus caused by activation of MAP kinase. *Nature* **376**, 58-62.

Vaillant, C., Michos, O., Orolicki, S., Brellier, F., Taieb, S., Moreno, E., Té, H., Zeller, R. and Monard, D. (2007). Protease nexin 1 and its receptor LRP modulate SHH signalling during cerebellar development. *Development* **134**, 1745-1754.

Watabe, T., Kim, S., Candia, A., Rothbacher, U., Hashimoto, C., Inoue, K. and Cho, K. W. (1995). Molecular mechanisms of Spemann's organizer formation: conserved growth factor synergy between Xenopus and mouse. *Genes Dev.* **9**, 3038-3050.

Yamada, S., Onishi, M., Fujinawa, R., Tadokoro, Y., Okabayashi, K., Asashima, M. and Sugahara, K. (2009). Structural and functional changes of sulfated glycosaminoglycans in Xenopus laevis during embryogenesis. *Glycobiology* **19**, 488-498.

Yu, S. R., Burkhardt, M., Nowak, M., Ries, J., Petrášek, Z., Scholpp, S., Schwille, P. and Brand, M. (2009). Fgf8 morphogen gradient forms by a source-sink mechanism with freely diffusing molecules. *Nature* **461**, 533-536.

Supplementary Material

The serpin PN1 is a feedback regulator of FGF signaling in germ layer and primary axis formation

Helena Acosta*, Dobromir Iliev*, Tan Hooi Min Grahn*, Nadège Gouignard, Marco Maccarana, Julia Griesbach, Svende Herzmann, Mohsen Sagha, Maria Climent, Edgar M. Pera

***) These authors equally contributed to this work.**

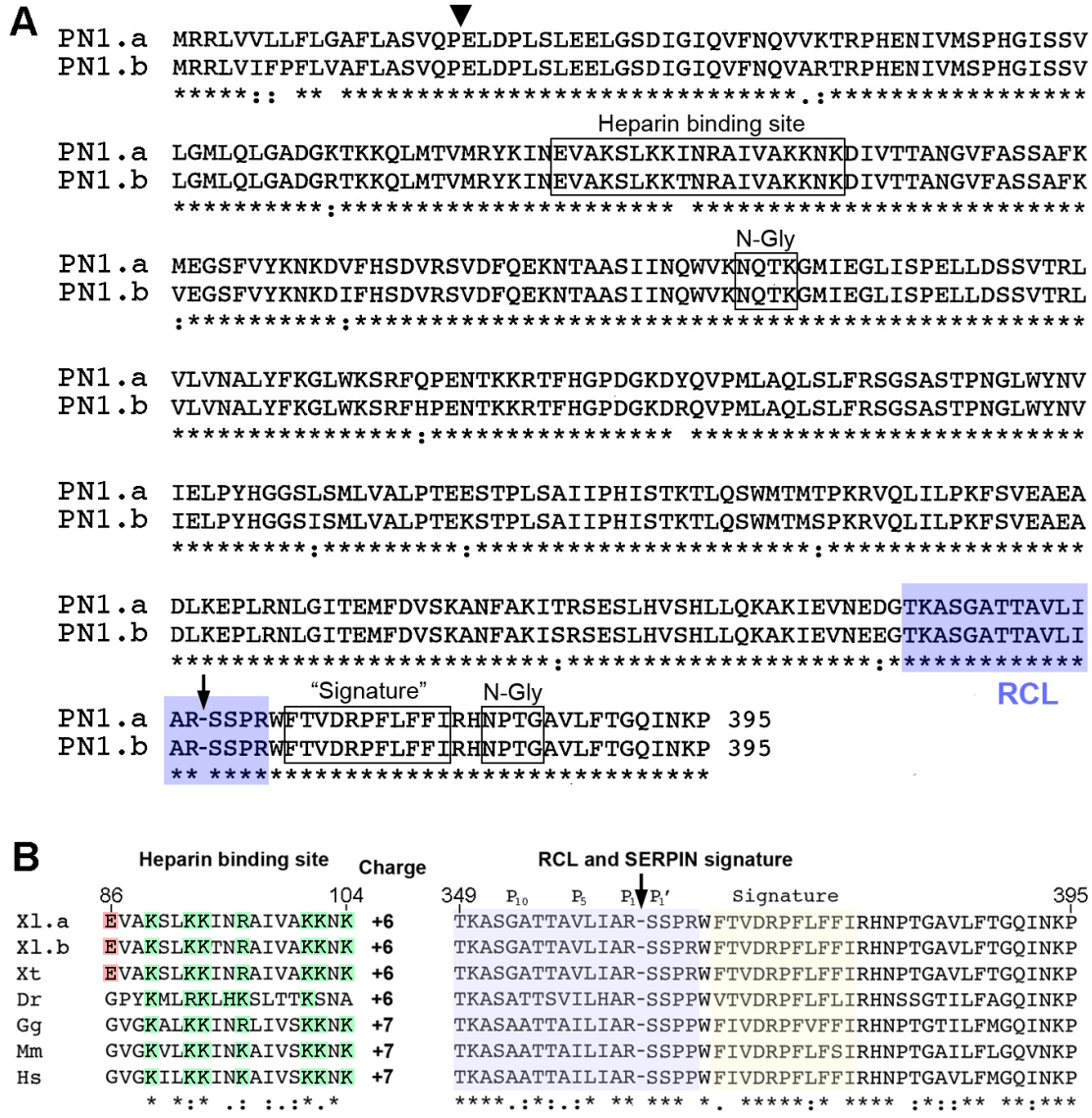

Figure S1. PN1 protein sequences

The alignment was performed using Clustal Omega multiple sequence alignment (EMBL-EBI) (Sievers et al., 2011). Identical amino acids are indicated with asterisks, similar residues with double points, and semi-conserved with single points. The RCL is indicated with a blue box and the SERPIN signature with a yellow box as determined by ScanProsite (http://prosite.expasy.org/scanprosite/) (Sigrist et al., 2010). The P1-P1' reactive site scissile bond in the RCL is indicated with a downward arrow (McGrogan et al., 1988).

(A) The signal peptide cleavage sites of *Xenopus laevis* PN1.a and PN1.b. were determined using SignalP 4.0 (Petersen et al., 2011) and are marked with an arrowhead. Boxes show the Heparin binding site (Stone et al., 1994) and the two N-Gly sites (predicted using the program NetNGlyc 1.0 Server (http://www.cbs.dtu.dk/services/NetNGlyc/). The numbers at the end of the sequences indicate the total length of the proteins. NCBI GenBank accession numbers are: PN1.a, DQ324047; PN1.b, BC077742. N-Gly, N-linked glycosylation; RCL, reactive center loop; SERPIN, serine protease inhibitor.

(B) Conserved functional domains of vertebrate PN1 proteins. Positive and negative amino acids in the heparin binding side are indicated in green and red, respectively. Px indicates amino acid positions in the RCL. Dr, zebrafish; Gg, chicken, Hs, human; Mm, mouse; Xl, African claw frog; Xt, Western clawed frog.

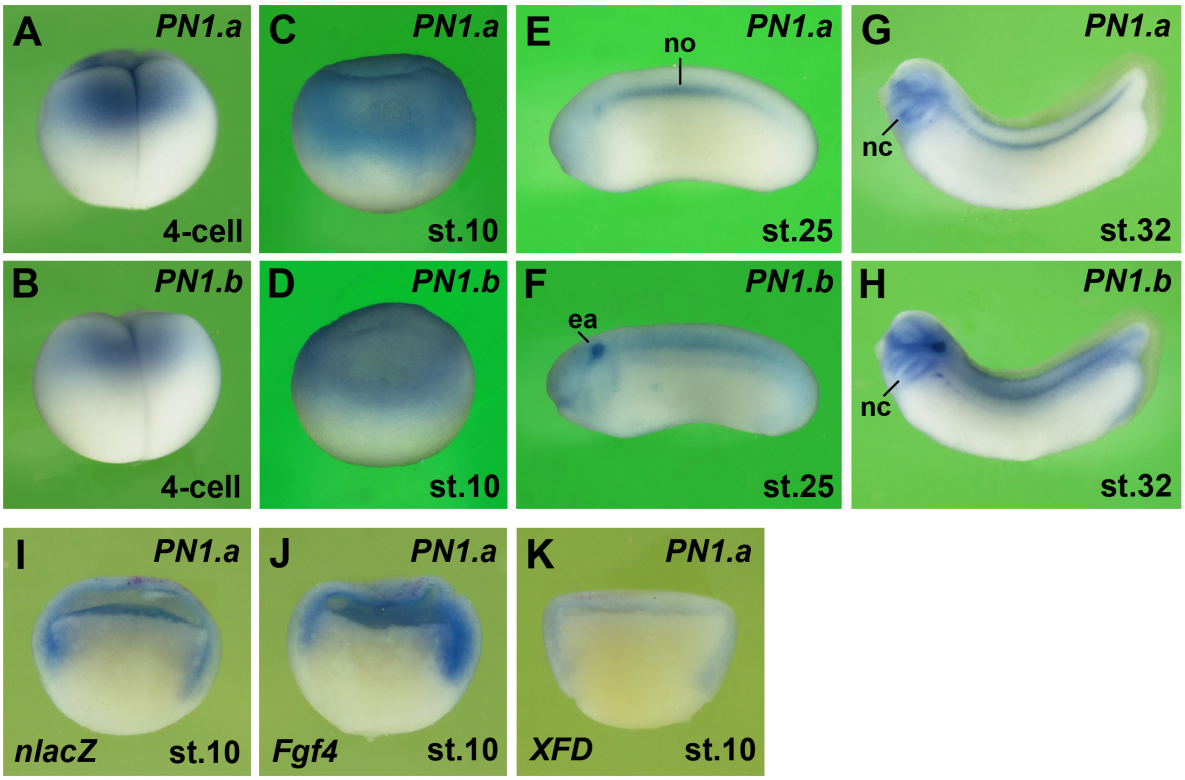

Figure S2. Gene expression and regulation of *PN1.a* and *PN1.b*

(A-H) Lateral view of uninjected *Xenopus* embryos after whole-mount *in situ* hybridization for *PN1.a* (upper row) and *PN1.b* (lower row).

(I-K) Hemi-sectioned gastrulae after a single injection of 9 pg *Fgf4* mRNA (J) and 450 pg *XFD* mRNA (K). 100 pg *nlacZ* mRNA was co-injected as lineage tracer (red nuclei).

ea, ear; nc, neural crest; no, notochord.

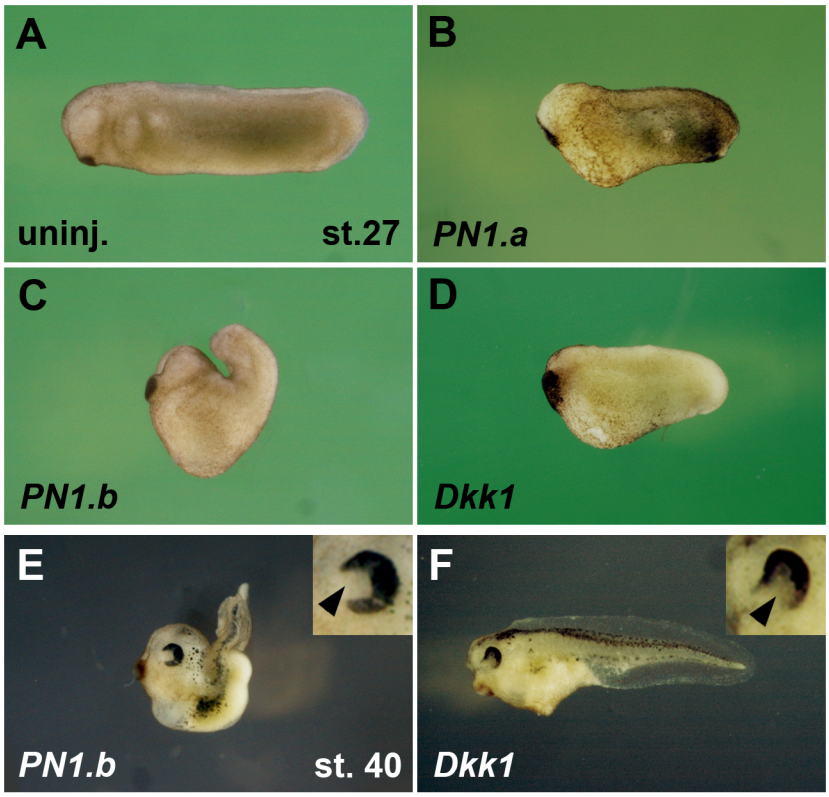

Figure S3. Overexpression of *PN1* and *Dkk1* promote anterior development

(A) Uninjected embryo at tailbud stage.

(B-D) *PN1.a*, *PN1.b*, and *Dkk1* mRNA induce enlarged head and shortened trunk/tail structures.

(E,F) *PN1.b* and *Dkk1* mRNA widen eye structures in tadpole embryos. Insets show magnification of eye. Note the expansion of the optic fissure (arrowhead) that is characteristic of coloboma.

Embryos were animally injected at the 4-cell stage with mRNAs: *PN1.a*, 4 ng; *PN1.b*, 16 ng; Dkk1, 32 pg. Indicated phenotypes were observed in B, 40/54; C, 23/23; D, 34/34; E, 26/31; F, 46/53.

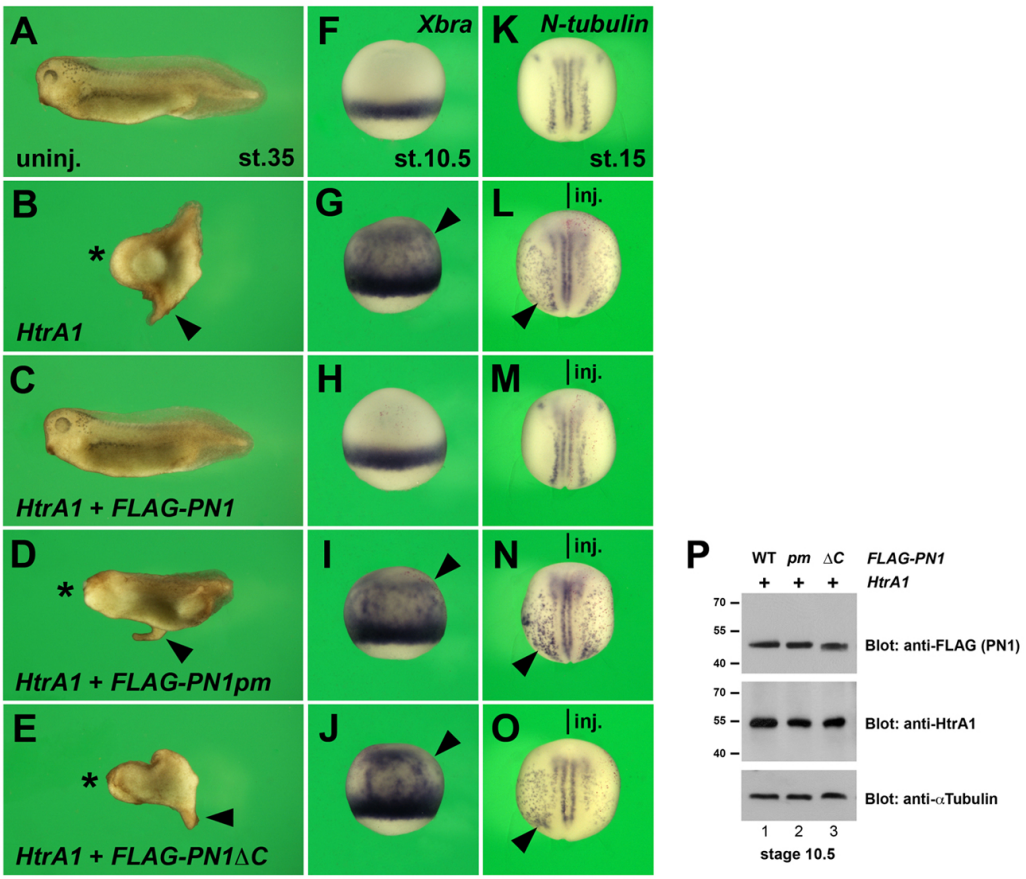

Fig. S4. PN1 inhibits via its RCL HtrA1-induced posteriorization, mesoderm induction, and neuronal differentiation

(A-E) *HtrA1* mRNA induces lack of head structures (asterisks) and secondary tail formation (arrowhead) at stage 35. Co-injection of *FLAG-PN1* mRNA restores normal head development and blocks ectopic tail outgrowth induced by *HtrA1* mRNA. *FLAG-PN1pm* has weak and *FLAG-PN1pm* mRNA no rescuing effect.

(F-O) *HtrA1* induces ectopic *Xbra* expression in the animal hemisphere (arrowhead in M) and ectopic *N-tubulin* expression in the lateral epidermis (arrowhead in R). *FLAG-PN1*, but not *FLAG-PN1pm* or *FLAG-PN1DC*, restore normal gene expression in *HtrA1*-injected embryos.

(P) Immunoblot analysis of embryos at stage 10.5 after co-injection of *HtrA1* and *FLAG-PN1*, *FLAG-PN1pm* or *FLAG-PN1DC* mRNA. α-Tubulin serves as a loading control. Note that FLAG-PN1, FLAG-PN1pm and FLAG-PN1ΔC proteins were expressed at equivalent levels, and that co-injected *HtrA1* mRNA produced comparable protein amounts in each sample.

Xenopus embryos were injected into a single blastomere with 100 pg *HtrA1*- and 300 pg *PN1*-derived mRNAs. Indicated phenotypes were: B, 21/22; C, 20/26; D, 16/26; E, 28/35; G, 53/53; H, 31/43; I, 26/46; J, 53/53; L, 55/55; M, 42/44; N, 35/41; O, 39/39.

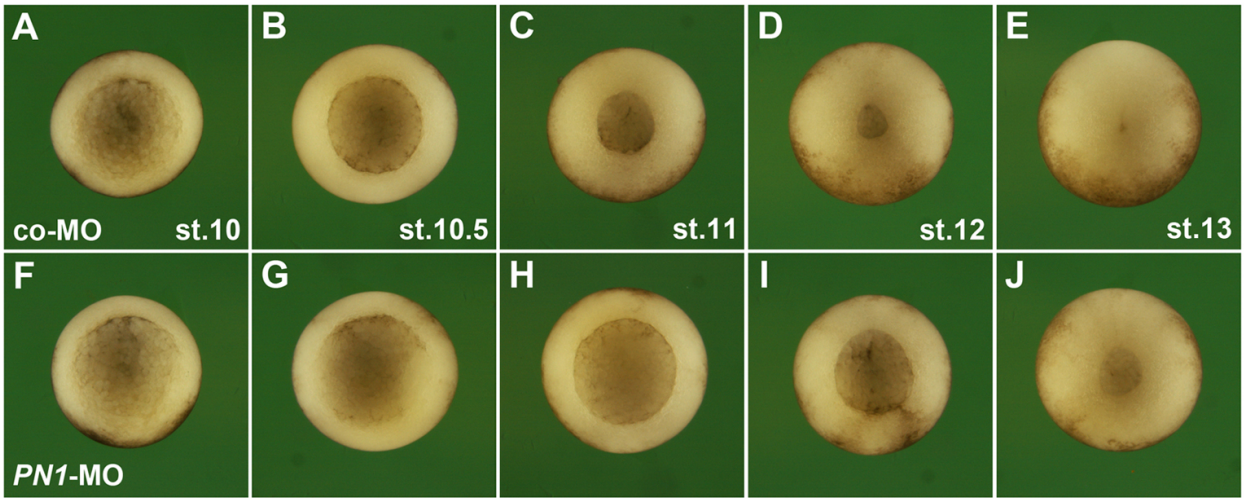

Figure S5. Knockdown of PN1 delays gastrulation

Embryos were animally injected with 60 ng MOs at the 4-cell stage. Embryos are shown in vegetal view, dorsal to the top, from the onset (left) to the end of gastrulation (right). Vertically aligned embryos are time-matched.

(A-E) Control-MO-injected embryos undergo normal gastrulation, which results in full closure of the circular blastopore.

(F-J) *PN1*-MO does not affect the onset of gastrulation at stage 10 (F), but causes a delay in blastopore closure at subsequent stages.

Pictures are representative of a minimum of 20 analysed embryos.

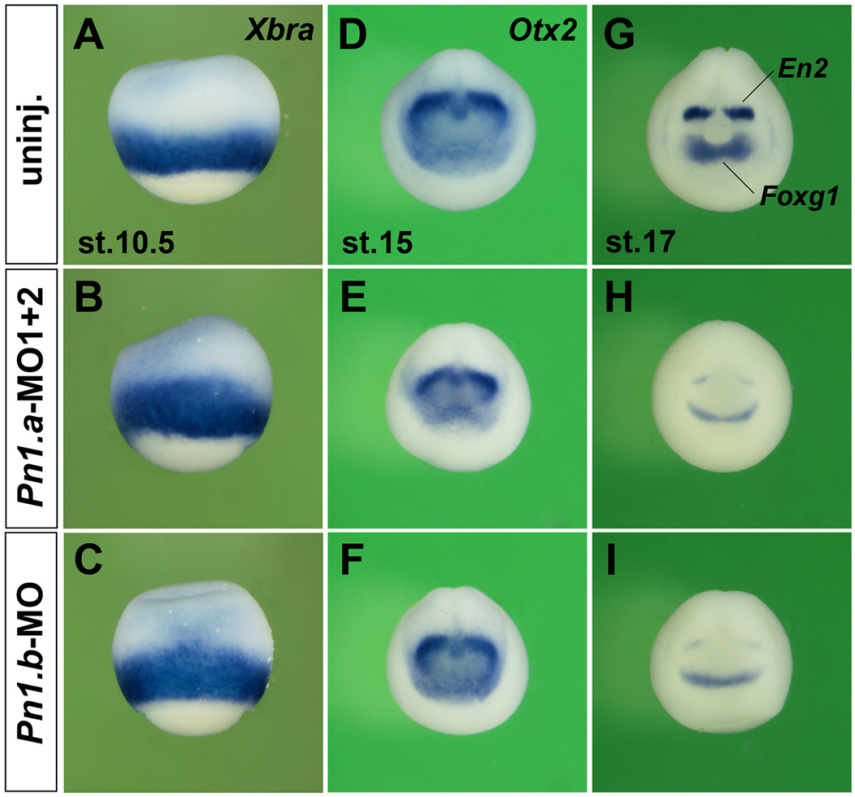

Figure S6. Downregulation of each *PN1* homeolog mildly stimulates mesoderm formation and reduces anterior development

Xenopus embryos were injected with a total of 60 ng MOs into the animal pole at the 4-cell stage. *PN1.a*-MO1+2 is an equal mixture of *PN1.a*-MO1 and *PN1.a*-MO2.

(A-C) Lateral view of early gastrula embryos after whole-mount *in situ* hybridization. Embryos injected with *PN1.a*-MO1+2 (B) or *PN1.b*-MO (C) exhibit a slight expansion of the mesodermal marker *Xbra* towards the animal pole.

(D-F) Anterior view of neurula embryos. Note the decreased expression domain of the anterior marker *Otx2* in embryos depleted of PN1.a (E) or PN1.b proteins (F).

(G-I) Anterior view of late neurulae. Embryos deficient for PN1.a (H) or PN1.b (I) show reduced expression of the telencephalic marker *Foxg1* and the posterior midbrain marker *En2*. Indicated phenotypes were observed in B, 19/19; C, 14/17; E, 11/11; F, 11/12; H, 12/15; I, 13/16.

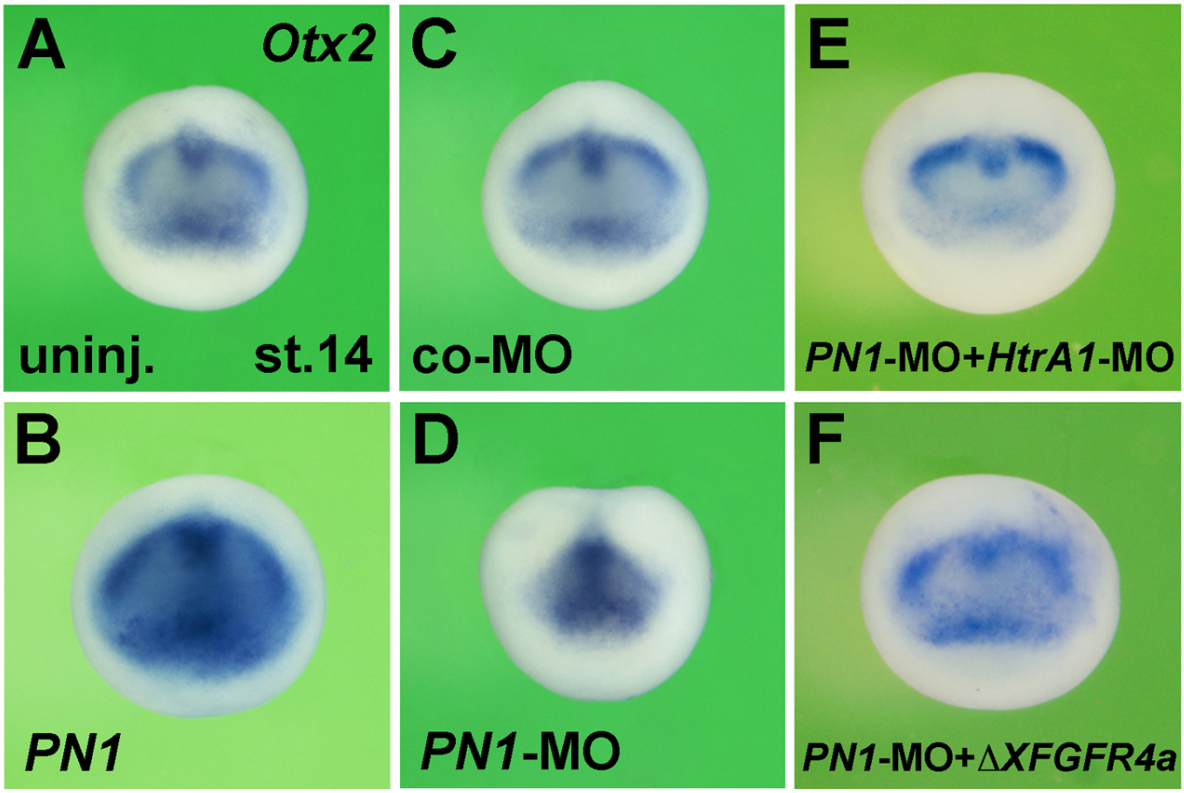

Figure S7. PN1 promotes anterior development via inhibition of HtrA1-, FGF- and Wnt signals

Embryos were animally injected with MOs at the 2-cell stage and mRNAs at the 4-cell stage.

(A) Anterior view of early neurula embryos after whole-mount *in situ* hybridization with *Otx2*, demarcating the prospective cement gland, forebrain and midbrain.

(B) *PN1* mRNA (4 ng) causes expansion of *Otx2* expression.

(C,D) *PN1*-MO (60 ng) reduces the *Otx2* marker, while an equivalent amount of control-MO has no effect.

(E,F) *HtrA1*-MO (20 ng) or 80 pg *ΔXFGFR-4a* mRNA restore normal *Otx2* expression in *PN1* morphant embryos.

Indicated phenotypes were observed in B, 12/13; C, 59/62; D, 63/73; E, 22/24; F, 23/29.

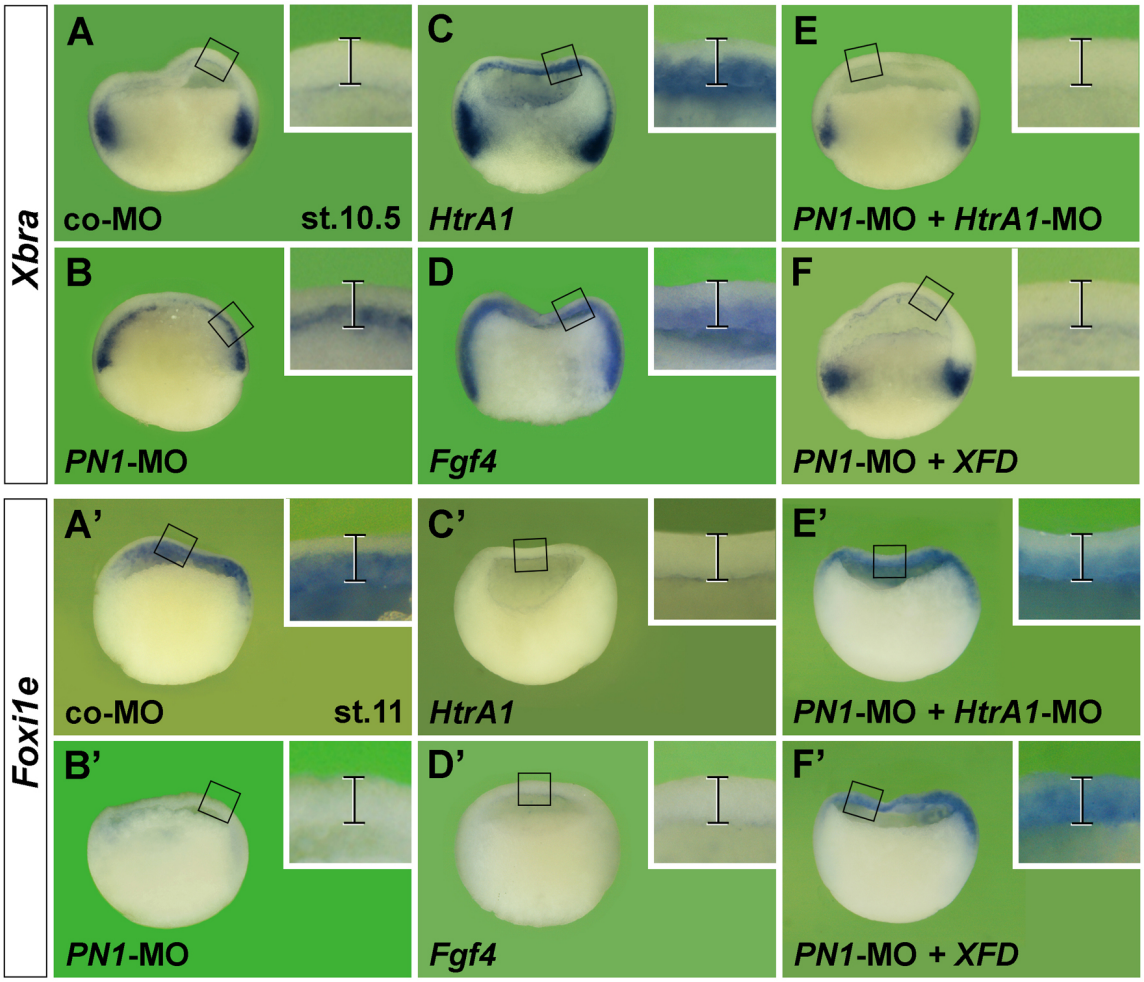

Figure S8. Knockdown of PN1 promotes mesoderm and suppresses ectoderm formation in an HtrA1- and FGF-dependent manner

Embryos were separately injected with MOs and mRNAs into the animal pole at the 4-cell stage. Hemisectioned early gastrula embryos are shown after whole-mount *in situ* hybridization for *Xbra* (A-F) and *Foxi1e* (A'-F').

(A-B') *PN1*-MO, but not control-MO, induces ectopic *Xbra* and reduction of *Foxi1e* expression in deep cells of the animal hemisphere (brackets in insets depict animal cap).

(C-D') Injections of 200 pg *HtrA1* and 2 pg *Fgf4* mRNA induce ectopic *Xbra* at the expense of *Foxi1e* expression in the inner layer of the animal cap (insets).

(E-F') Injections of *HtrA1*-MO and 80 pg *XFD* mRNA restore normal expression of *Xbra* and *Foxi1e* in *PN1*-morphant embryos.

Total injected MO amount was 60 ng (+20 ng *HtrA1*-MO). The frequency of the indicated phenotypes was A, 136/144; A', 50/59; B, 148/177; B', 50/69; C, 21/21; C', 47/57; D, 79/79; D', 93/97; E, 66/90; E', 52/56; F, 72/83; F', 45/51.

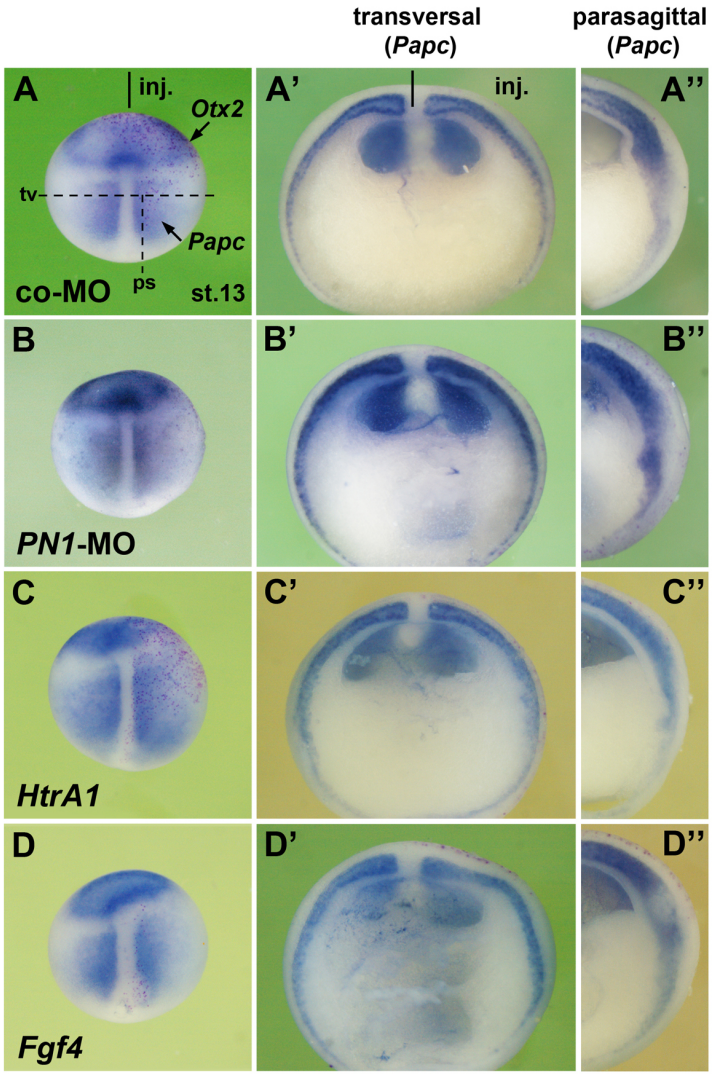

Figure S9. P*N1*-MO, *HtrA1*, and *FGF4* do not induce ectopic *Papc* expression in the ectoderm of post-gastrula embryos.

Embryos were animally injected into a single blastomere at the 4-cell stage with *nlacZ* mRNA as a lineage tracer (red nuclei) and processed for whole-mount *in situ* hybridization for *Otx2* and *Papc*.

(A-A'') Embryo injected with 15 ng control-MO. Strippled lines in dorsal view of neurula embryo indicate section planes. Note *Papc* expression in transversally sectioned trunk mesoderm (A') and parasagitally sectioned tailbud mesoderm (A'').

(B-D'') *PN1*-MO (15 ng), *HtrA1* mRNA (50 pg), and *Fgf4* mRNA (0.5 pg) shift the *Otx2*-*Papc* border anteriorwards (B-D), but fail to induce ectopic *Papc* expression in the overlying ectoderm on the injected right side (B'-D'').

The frequency of the indicated phenotypes was A, 79/79; A'+A'', 4/4; B, 47/57; B'+B'', 13/13; C, 93/97; C'+C'', 8/8; D, 12/13; D'+D'', 8/9.

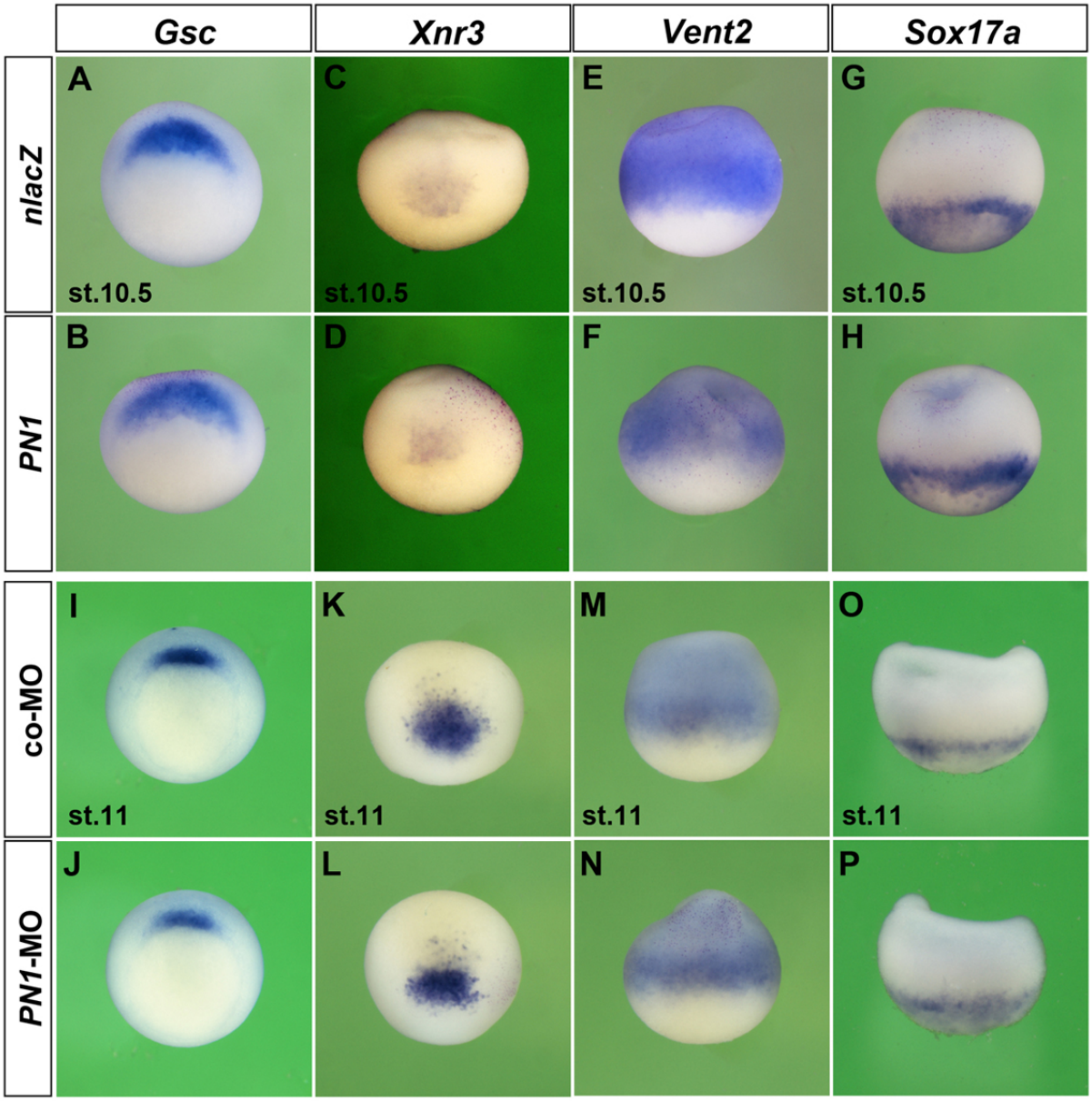

Figure S10. Overexpression or knockdown of *PN1* does not affect expression of *Gsc*, *Xnr3*, *Vent2*, and *Sox17a*

Whole-mount *in situ* hybridization of *Xenopus* embryos at early gastrula stage in vegetal (A,B,I,J) and lateral view (C-H, K-P). Embryos were injected into the margin (A-H) or animal pole (K-N) of a single blastomere at the 4-cell stage with *nlacZ* mRNA as lineage marker (red nuclei). Embryos in (I,J) were animally and in (O,P) marginally injected. Injected doses per embryo were: *nlacZ* mRNA (100 pg), *PN1* mRNA (4 ng), MOs (15 ng in K-N; 60 ng in I,J,O,P). *PN1*-MO is an equal mixture of *PN1.a*-MO1, *PN1.a*-MO2, and *PN1.b*-MO.
(A,B,I,J) *Gsc* expression in the dorsal mesoderm.
(C,D,K,L) *Xnr3* expression in the dorsal mesoderm.
(E,F,M,N) *Vent2* expression in the ventrolateral mesoderm and ventral ectoderm.
(G,H,O,P) *Sox17a* expression in the endoderm.
Indicated phenotypes were observed in A, 8/8; B, 15/15; C, 7/7; D, 8/8; E, 11/11; F, 14/19; G, 14/14; H, 25/25; I, 11/11; J, 15/15; K, 9/9; L, 10/10; M, 12/12; N, 18/18; O, 30/30; P, 26/26.

Table S1. Antisense morpholino oligonucleotides (all from Gene Tools LLC.)

Gene	Forward	Reference
control-MO (standard)	5'- CCT CTT ACC TCA GTT ACA ATT TAT A	Gene Tools LLC.
random-MO	not specified	Gene Tools LLC.
PN1.a-MO1	5'- GAA GTC AAG TAA GAA TAC TCC CGG C	This study
PN1.a-MO2	5'- ACT AGT CGC CTC ATG ATC GTA CAA C	This study
PN1.b-MO	5'- CAT GAT CGT AGA ACT GGA TAG AAG T	This study
PN1-5mm-MO	5'-ACT ACT CAC CTA ATG ATA GTA AAA C	This study
HtrA1-MO	5'- ACA CCG CCA GCC ACA ACA TGG TCA T	Hou et al., 2007

Table S2. Oligonucleotides for RT-PCR

Gene	Forward	Reverse	Tm/ °C	Cycles
Histone H4	5'-CGG GAT AAC ATT CAG GGT ATC ACT	5'-CAT GGC GGT AAC TGT CTT CCT	50	25
PN1.a	5'-CGT GAT CCT TCA CAT GGG GT	5'-GTA GCC CTT CAG CTG TCC TG	57	27
PN1.b	5'-TTG GCA AAG CAA CAT CCG TG	5'-CAA GGG CAG CGA CTC AAA TG	55	27
HtrA1	5'-TGT TGT GGC TGG CGG TGT TAC TG	5'-TCC ATC CTC CGA CAC AAT GAA TCC	57	43

2. Supplementary Materials and Methods

2.1 Expression constructs

A full length cDNA clone of *X. laevis PN1.a* (=*PN1*) in pcDNA3 was isolated by secretion cloning (Pera et al., 2005) and corresponds to an NCBI sequence entry (GenBank accession number DQ324047). The insert was subcloned into pCS2 to generate pCS2-*PN1*. The open reading frame of *PN1* including 64 upstream nucleotides of the 5'UTR was fused with a FLAG-tag at the C-terminus to construct pCS2-*PN1-FLAG*. The open reading frame of PN1 lacking the signal peptide but including the Chordin leader peptide followed by a FLAG-tag at the N-terminus was subcloned to generate pCS2-*FLAG-PN1* and used as template to construct pCS2-*FLAG-PN1pm* (*R362P*, *S363P*), pCS2-*FLAG-PN1ΔC* (deletion of amino acids 349-395), and pCS2-*HA-PN1* (substitution of the FLAG-tag by an HA-tag). A full length cDNA clone of *X. laevis PN1.b* in pCMVSport6 was obtained from Source Bioscience LifeSciences, Cambridge, UK (GenBank accession number BC077742). The open reading frame of *PN1.b* including 41 upstream nucleotides of the 5'UTR was fused with a FLAG-tag at the C-terminus to construct pCS2-*PN1.b-FLAG*. pCS-*HtrA1* (Hou et al., 2007) was used as template to generate pCS2-*HtrA1ΔN* (deletion of amino acids 24-150). A Myc tag was fused to the C-terminus of the HtrA1 open reading frame to construct pCS2-*HtrA1-Myc* and used as template to generate pCS2-*HtrA1-ΔPDZ-Myc* (deletion of amino acids 359-457).

2.2 Microinjection

To prepare sense RNA, all pCS2 constructs containing *HtrA1ΔTrypsin* and *HtrA1(S307A)* (Hou et al., 2007), *Fgf4* (Isaacs et al., 1994), and *FLAG-Sdc4* (Muñoz et al., 2006) were linearized with *Not*I and transcribed with Sp6 RNA polymerase (mMessage Machine, Ambion). p*XFD/Xss* (*Eco*RI linearization; Amaya et al., 1991) and pXEX-*nlacZ* (*Xba*I linearization; a kind gift of R. Harland, UC Berkeley, USA) were transcribed with T7 polymerase. pSP64T-*ΔXFGFR-4a* (*Sal*I linearization; Hongo et al., 1999) was transcribed with Sp6 RNA polymerase. *PN1.a* and *Wnt3a* (Saint-Jeannet et al., 1997) cDNAs were microinjected as non-digested pCS2 expression plasmids.

2.3 Immunoprecipitation and immunoblotting

Immunoprecipitation was done as described (Hou et al., 2007). Cleared lysates from 100 embryos containing 10 mg of extracted proteins were incubated in 100 μl agarose A/G beads

(Santa Cruz) coupled to 45 μg anti-HtrA1, 30 μg anti-Flag (AbD Serotec, 4497-1010), and 10 μg anti-Myc (Santa Cruz, sc-47694) antibodies. For immunoblotting, 10 embryos were lysed in 100 μl lysis buffer (50 mM Tris pH 7.4, 150 mM NaCl, 1 mM EDTA, 0.5% Triton X-100, and protease inhibitor cocktail). For pSmad proteins, the lysis buffer was complemented with phosphatase inhibitor cocktail. Proteins were separated by SDS-PAGE and exposed to the following antibodies: immuno-purified anti-*Xenopus* PN1 (20 μg/ml), immuno-purified anti-*Xenopus* HtrA1 (5 μg/ml; Hou et al., 2007), anti-pSmad2 (1:1000, Cell Signaling, 3101), anti-pSmad1/5/8 (1:1000, Cell Signaling, 9511), anti-Flag M2-peroxidase (1:2000, Sigma, A8592), anti-HA (1:2000, Sigma), and anti-alpha-tubulin (1:2000; Sigma, T9026).

3. Supplementary References

McGogan M., Kennedy J., Li M. P., Hsu C., Scott R. W., Simonsen C. C. and Baker J. B. (1988). Molecular cloning and expression of two forms of human protease Nexin 1. Nature *Biotechnology* **6**, 172-177.

Petersen T. N., Brunak S., von Heijne G. and Nielsen H. (2011). SignalP 4.0: discriminating signal peptides from transmembrane regions. *Nature Methods* **8**, 785-786.

Saint-Jeannet J.P., He X., Varmus H.E. and Dawid I.B. (1997). Regulation of dorsal fate in the neuraxis by Wnt-1 and Wnt-3a. *Proc. Natl. Acad. Sci. U S A* **94**, 13713-13718.

Sievers F., Wilm A., Dineen D. G., Gibson T. J., Karplus K., Li W., Lopez R., McWilliam H., Remmert M., Söding J., Thompson J. D. and Higgins D. G. (2011). Fast, scalable generation of high-quality protein multiple sequence alignments using Clustal Omega. *Molecular Systems Biology* **7**, 539 doi:10.1038/msb.2011.75

Sigrist C. J., Cerutti L., de Castro E., Langendijk-Genevaux P. S., Bulliard V., Bairoch A. and Hulo N. (2010). PROSITE, a protein domain database for functional characterization and annotation. *Nucleic Acids Res.* **38** (Database issue):D161-6.

Stone S. R., Brown-Luedi M. L., Rovelli G., Guidolin A., McGlynn E. and Monard D. (1994). Localization of the heparin-binding site of glia-derived nexin/protease nexin-1 by site-directed mutagenesis. *Biochemistry* **33**, 7731-5.